JAN 30 1956 REC'D

CONFIDENTIAL

Copy 1
RM SL56A11

CLASSIFICATION CANCELLED
Authority NASA PUBLICATIONS ANNOUNCEMENTS NO. 7
Date 6/30/59 By

PERMANENT FILE COPY

NACA

RESEARCH MEMORANDUM

for the

Bureau of Aeronautics, Department of the Navy

STATIC LONGITUDINAL AND LATERAL STABILITY AND CONTROL DATA OBTAINED FROM TESTS OF A 1/15-SCALE MODEL OF THE GOODYEAR XZP5K AIRSHIP

TED NO. NACA DE 211

By Michael D. Cannon

Langley Aeronautical Laboratory
Langley Field, Va.

CLASSIFIED DOCUMENT

This document contains classified information affecting the National Defense of the United States within the meaning of the Espionage Act, USC 18:793 and 794. Its transmission or the revelation of its contents in any manner to an unauthorized person is prohibited by law.

NATIONAL ADVISORY COMMITTEE
FOR AERONAUTICS

WASHINGTON

JAN 25 1956

FILE COPY
To be returned to
the files of the National
Advisory Committee
for Aeronautics
Washington, D. C.

20

CLASSIFICATION CANCELLED
Authority NASA PUBLICATIONS ANNOUNCEMENTS NO.
Date By

CONFIDENTIAL

NASA Technical Library
3 1176 01438 9754

UNCLASSIFIED

NATIONAL ADVISORY COMMITTEE FOR AERONAUTICS

RESEARCH MEMORANDUM

for the

Bureau of Aeronautics, Department of the Navy

STATIC LONGITUDINAL AND LATERAL STABILITY AND CONTROL DATA OBTAINED FROM TESTS OF A 1/15-SCALE MODEL OF THE GOODYEAR XZP5K AIRSHIP

TED NO. NACA DE 211

By Michael D. Cannon

SUMMARY

Static longitudinal and lateral stability and control data are presented of an investigation on a 1/15-scale model of the Goodyear XZP5K airship over a pitch and yaw range of $\pm 20^{\circ}$ and 0° to 30°, respectively, for various rudder and elevator deflections. Two tail configurations of different plan forms were tested and wake and boundary-layer surveys were conducted. Testing was conducted in the Langley full-scale tunnel at a Reynolds number of approximately 16.5×10^6 based on hull length, and corresponds to a Mach number of about 0.12.

INTRODUCTION

Current requirements for the use of airships in antisubmarine operations call for maneuver rates substantially higher than those used in past years. These maneuvers result in operation at high pitch and yaw attitudes which has caused some tail surface failures in service operations and which introduces new design problems for future airship configurations. Since the existing airship-loads data available for design purposes are limited to low-aspect-ratio surfaces and relatively low airship attitude ranges, the Bureau of Aeronautics, Department of the Navy, requested that a fin-loads investigation be conducted on a 1/15-scale model of the Goodyear XZP5K airship in the Langley full-scale wind tunnel.

CONFIDENTIAL
UNA Restriction/Classification Cancelled
UNCLASSIFIED

Tests were conducted for two types of tail surfaces representing current designs. Although the primary objective of the investigation was to obtain extensive fin-loads pressure data, model force data were also obtained over a pitch range of $\pm 20^{\circ}$ at yawed attitudes up to 30° for a full range of elevator and rudder deflections from which some of the static longitudinal and lateral stability derivatives can be determined. Also included were limited boundary-layer surveys and wake momentum surveys at the rear of the body to provide some data for stern propulsion design studies.

This paper presents only the model force test data and the boundary-layer and wake survey measurements. These data are presented without analysis to expedite publication.

SYMBOLS AND COEFFICIENTS

Force and moment coefficients are based on hull volume as in reference 1 and are referred to the stability axes the origin of which is the center of buoyancy. This point is located on the model center line $0.456l$ back of the nose.

C_L lift coefficient, $\frac{\text{Lift}}{q_o(V)^{2/3}}$

$C_{D'}$ drag coefficient, $\frac{\text{Drag}}{q_o(V)^{2/3}}$

C_Y side-force coefficient, $\frac{\text{Side force}}{q_o(V)^{2/3}}$

C_m pitching-moment coefficient, $\frac{\text{Pitching moment}}{q_o V}$

C_n yawing-moment coefficient, $\frac{\text{Yawing moment}}{q_o V}$

C_l rolling-moment coefficient, $\frac{\text{Rolling moment}}{q_o V}$

V volume of hull, 192.8 ft^3

l	length of hull, 18.79 ft
q_o	free-stream dynamic pressure, $\rho U^2/2$, lb/ft^2
q	local dynamic pressure, $\rho u^2/2$, lb/ft^2
ρ	mass density of air, $lb\text{-}sec^2/ft^4$
U	free-stream velocity, ft/sec
u	local velocity, ft/sec
α	angle of pitch, positive when nose up, deg
ψ	angel of yaw, positive when nose to right, deg
δ_r	rudder angle, positive when trailing edge deflected to left, deg
δ_{e_L}	left elevator angle, positive when trailing edge deflected down, deg
R	Reynolds number, based on hull length
δ_{e_R}	right elevator angle, positive when trailing edge deflected down, deg

MODEL

The model used for this investigation was a 1/15-scale model of the Goodyear XZP5K airship. This corresponds to a model length of 18.79 feet and a volume of 192.8 cubic feet. Figure 1 shows the model installed in the tunnel and figure 2 presents some of the more pertinent geometric characteristics of the hull.

Two sets of tails were used in the investigation. Both sets were inverted Y-tail arrangements with a radial spacing of 120° between fins, but differed in plan form and area. The first, designated the standard tail, was of the conventional low-aspect-ratio design having a rudder area approximately 24 percent of the total area. The second, designated the high-aspect-ratio tail, was smaller in area and had a rudder area approximately 45 percent of its total area. Plan forms and pertinent geometric characteristics of the two tail configurations are shown in figures 3 and 4. All control surfaces were equipped with actuators allowing independent deflection of each control surface through a range of ±40°.

TESTS

Force test data were obtained for both the standard and high-aspect-ratio-tail configurations over a pitch range of $\pm 20^{\circ}$ for yawed attitudes from 0° to 30°. The rudder and left elevator controls were deflected independently $\pm 40^{\circ}$ for all model attitudes to provide separate effectiveness evaluation of each control. For the purpose of this report the rudder is considered the control surface of the top fin and the elevator the control surface of the side fins.

Measurements of the boundary-layer profile were made along the top and side center line of the hull at $0.60l$, $0.75l$, and $0.97l$ through the complete pitch range at zero yaw, and wake momentum surveys were conducted at yaw angles of 0° and 21° immediately in the rear of the hull. A region of approximately 42 inches square was surveyed.

The tests were conducted at a Reynolds number of approximately 16.5×10^6 based on hull length and corresponds to a Mach number of about 0.12. From consideration of model surface conditions, general tunnel turbulence, and high R, the hull boundary layer in the region of the tails would be expected to be turbulent in nature.

CORRECTIONS

All data presented in this paper have been corrected for tunnel stream angle and model buoyancy effects. Strut tare corrections have also been applied to all data, based on tare evaluations made using the image system at the zero yaw condition. Time did not permit such evaluations at yaw conditions and it should be noted that the zero yaw tares are probably conservative when applied to the highly yawed conditions.

PRESENTATION OF DATA

As stated in the introduction, these data are presented without analysis to expedite publication. This treatment is prompted by the specific nature of the tests.

The data of this investigation are presented as follows:

	Figure
Longitudinal characteristics of the model with controls neutral for various yaw angles. (Standard and high-aspect-ratio tails installed).	5 and 6

Figure

Effect of elevator deflection on longitudinal characteristics for various pitch and yaw angles. (Standard and high-aspect-ratio tails installed) . . . . . 7 and 8

Lateral characteristics of the models with controls neutral for various pitch angles. (Standard and high-aspect-ratio tails installed) 9

Effect of rudder deflection on lateral characteristics for various pitch and yaw angles. (Standard tail installed) . . . 10

Effect of elevator deflection on lateral characteristics for various pitch and yaw angles. (Standard tail installed) . . . 11

Effect of rudder deflection on the lateral characteristics for various pitch and yaw angles. (High-aspect-ratio tail installed) 12

Effect of elevator deflection on the lateral characteristics for various pitch and yaw angles. (High-aspect-ratio tail installed) 13

Boundary-layer-velocity profiles along the top and side hull center line for various pitch angles. 14

Dynamic pressure surveys in the region of the tail cone at angles of yaw of 0° and 21°. . . . . 15 and 16

Profile irregularities noted in figure 14 at high angles of attack are probably due to the large relative angle between the local stream angle and survey rake. In the 0.97l position interference is likely from the tail surfaces.

The fin wakes are clearly defined for the zero angle of yaw case, figure 15, and the contours appear adequately defined. The break in contours in the lower middle portion marks the strut location. For an angle of yaw of 21°, figure 16, however, a considerable wake confused

the pressure profiles. At least the order of magnitude of gross wake influence is shown, although the strut wake is swept to the lower right and mixed in with the body wake.

Langley Aeronautical Laboratory,
National Advisory Committee for Aeronautics,
Langley Field, Va., January 11, 1956.

Michael D. Cannon
Aeronautical Research Scientist

Approved: Eugene C. Draley
Eugene C. Draley
Chief of Full-Scale Research Division

JBB

REFERENCE

1. Freeman, Hugh B.: Force measurements on a 1/40-Scale Model of the U. S. Airship "Akron." NACA Rep. 432, 1932.

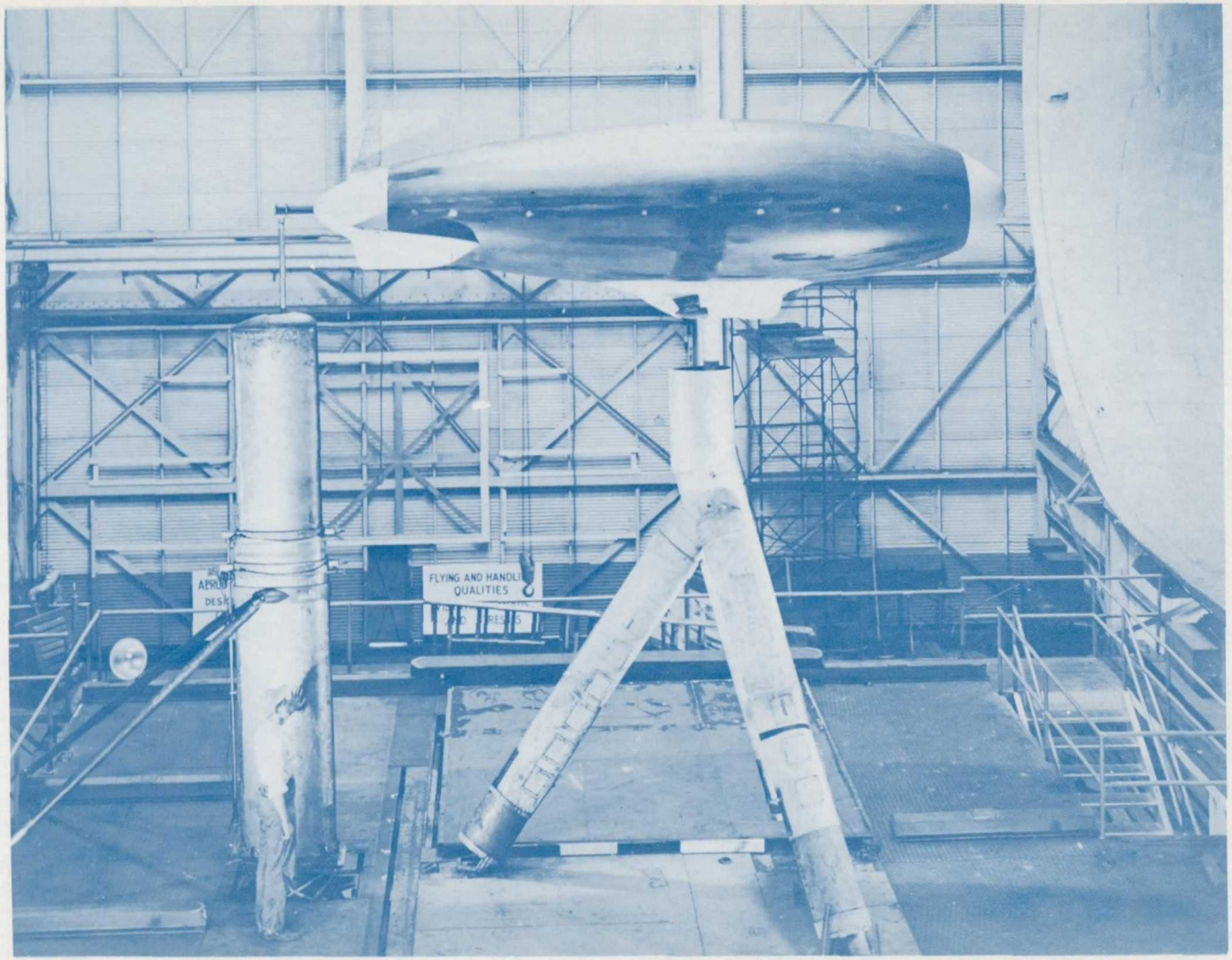

L-85370

Figure 1.- General view of Goodyear XZP5K airship model with the standard tail installed.

Figure 2.- Geometric characteristics of airship model hull. Dimensions are in inches.

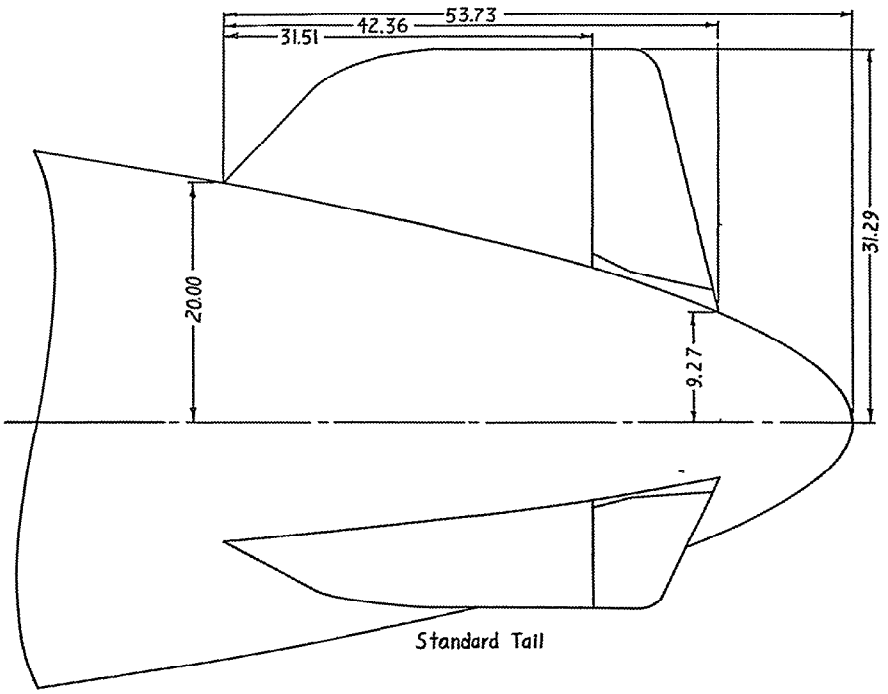

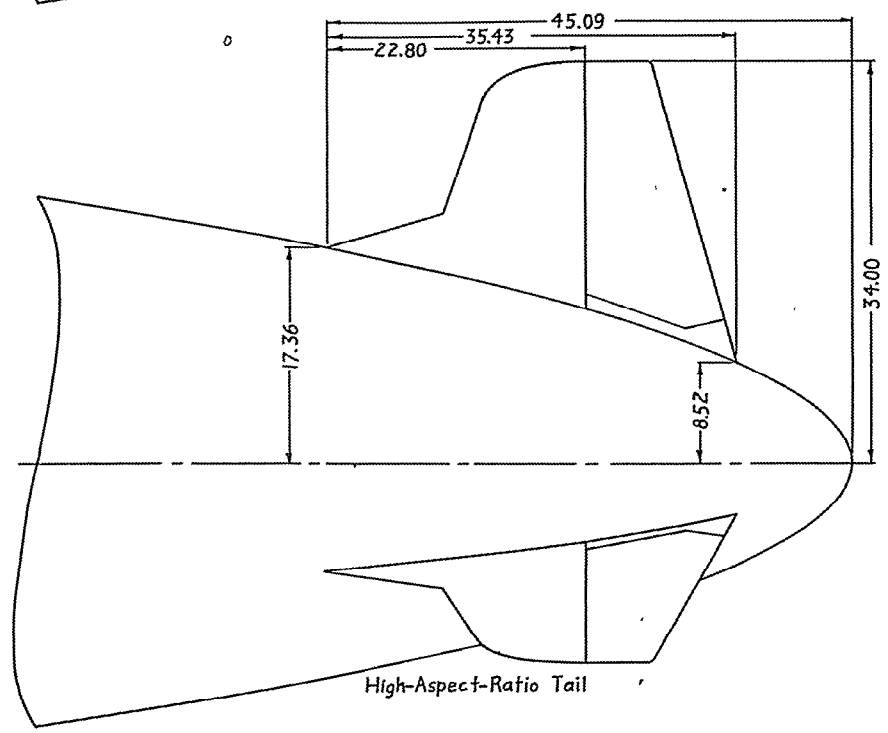

TYPE of TAIL	CONTROL AREA	FIN AREA
STANDARD	.92	3.82
HIGH-ASPECT RATIO	1.36	3.03

gure 3.- Sketch of standard and high aspect ratio tails. Dimensions are in inches.

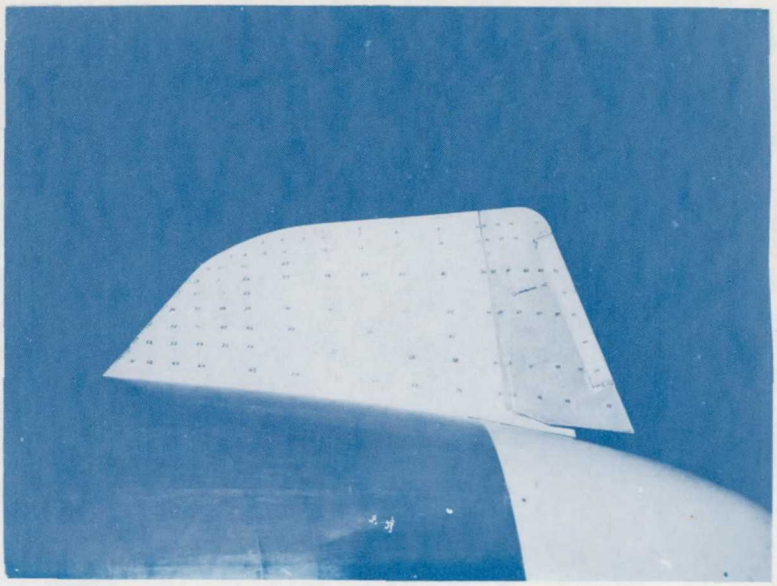

Standard tail L-85375

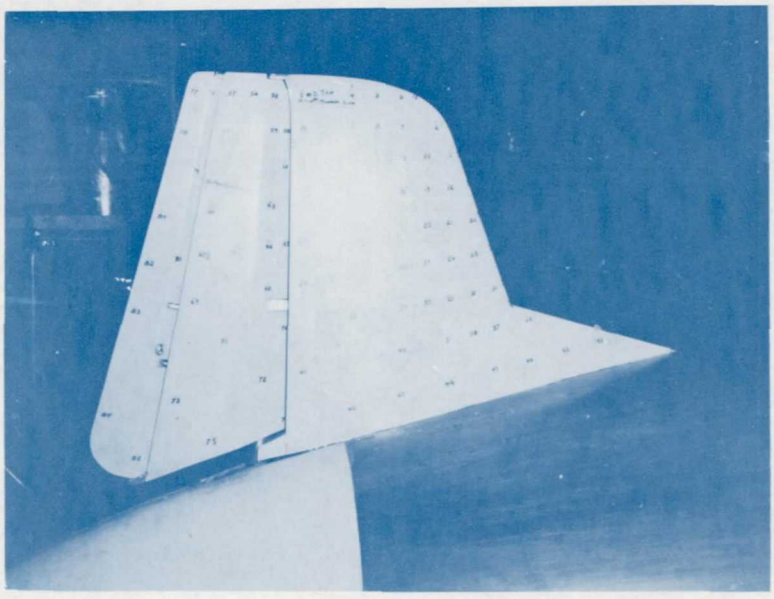

High-aspect-ratio tail L-85571

Figure 4.- Top fin of each tail configuration.

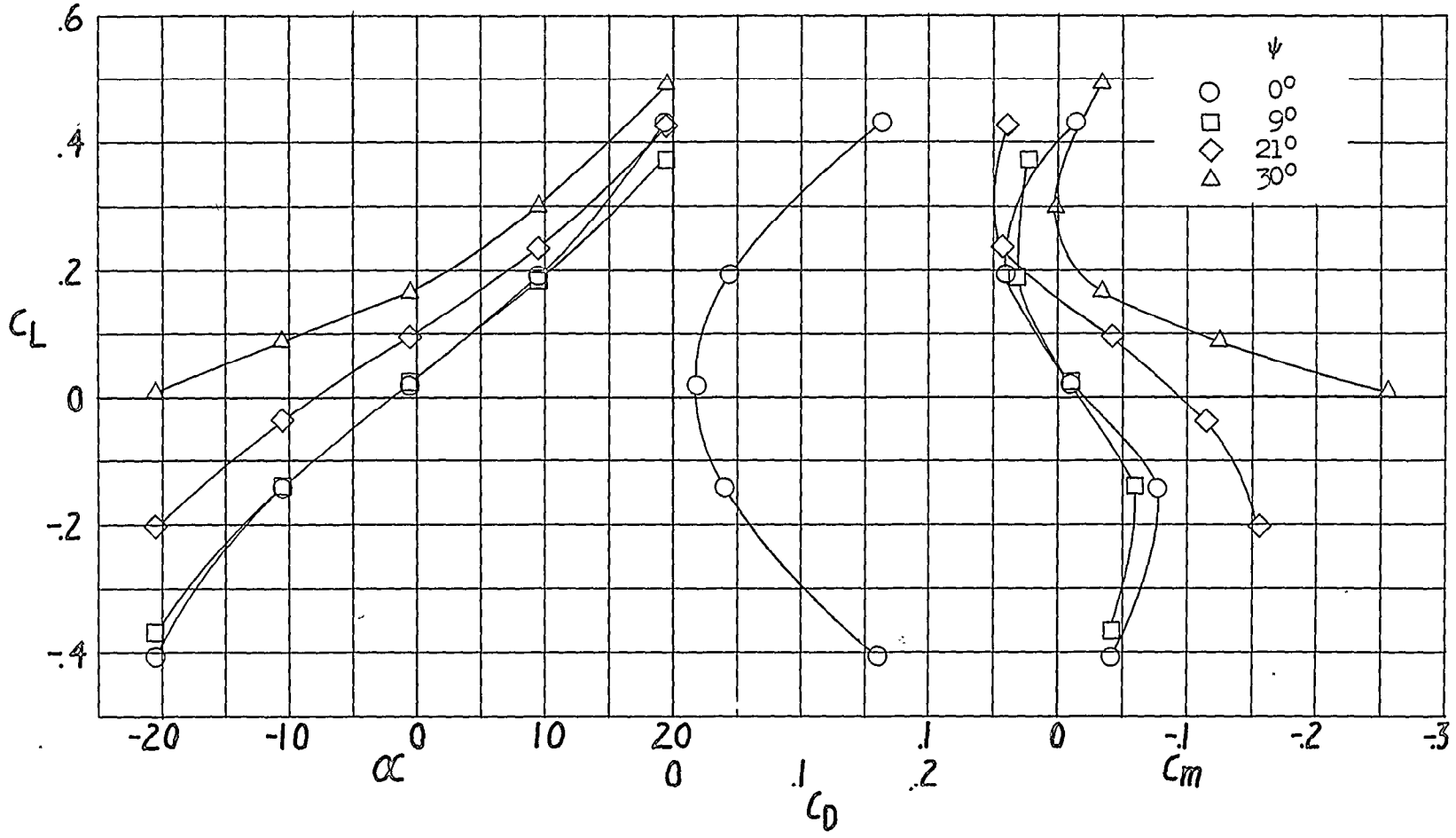

Figure 5.- Longitudinal characteristics of the Goodyear XZP5K airship model. Standard tail installed; $\delta_r = 0^\circ$; $\delta_{e_L} = 0^\circ$; $\delta_{e_R} = 0^\circ$.

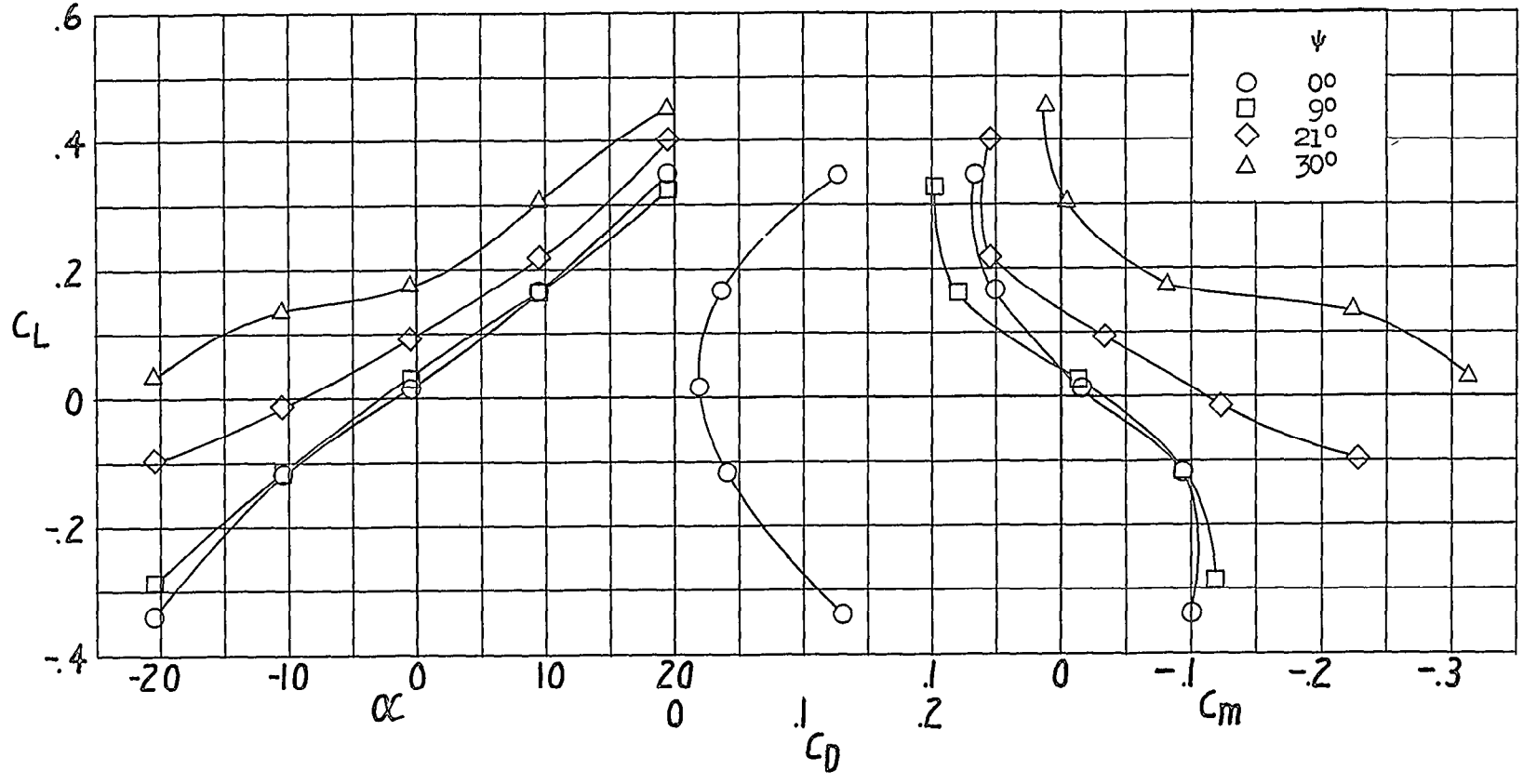

Figure 6.- Longitudinal characteristics of the Goodyear XZP5K airship model. High-aspect-ratio tail installed; $\delta_r = 0°$; $\delta_{e_L} = 0°$; $\delta_{e_R} = 0°$.

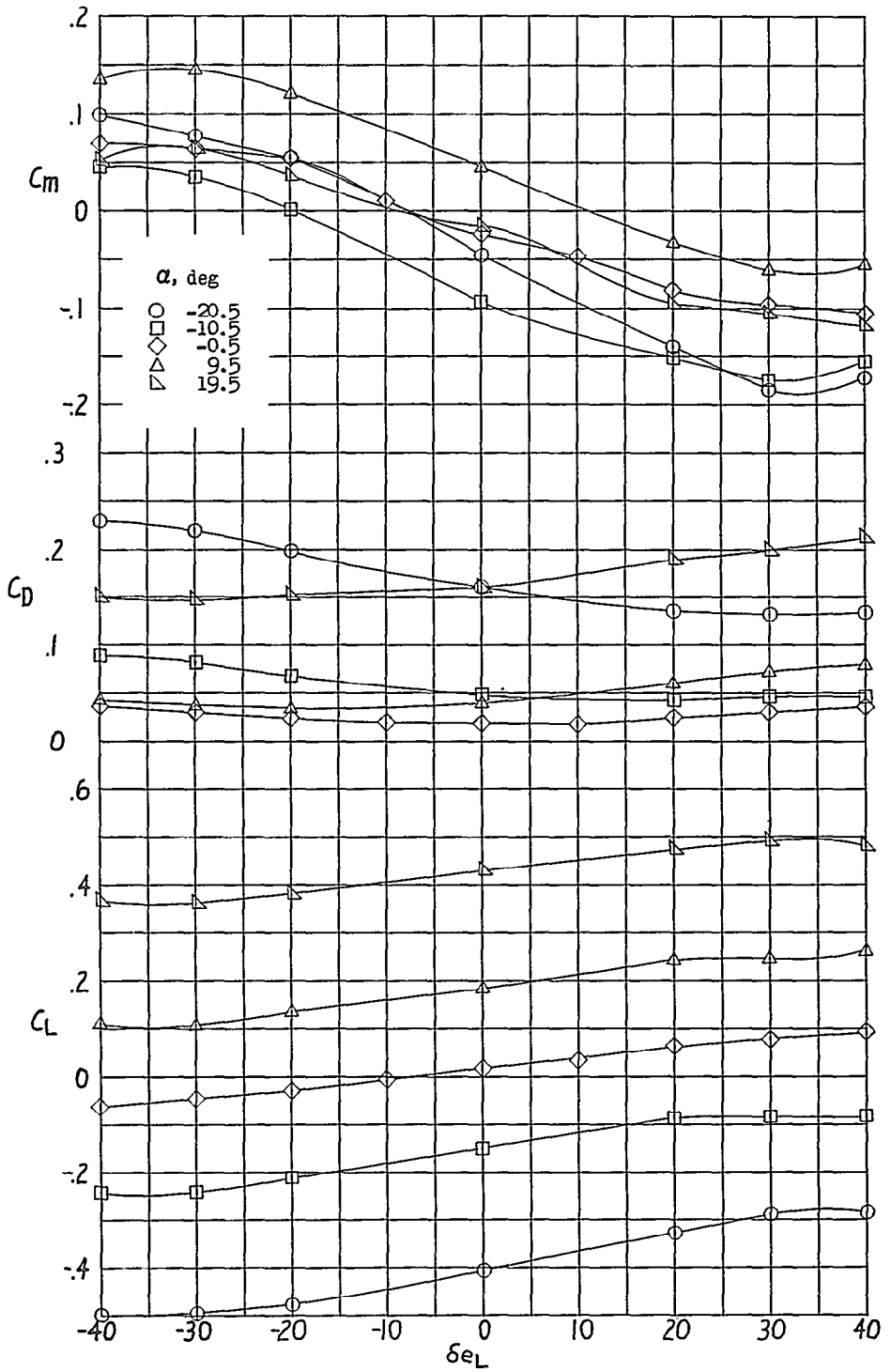

(a) $\psi = 0^\circ$.

Figure 7.- Effect of left elevator deflection on the longitudinal characteristics. Standard tail installed; $\delta_r = 0^\circ$; $\delta_{e_R} = 0^\circ$.

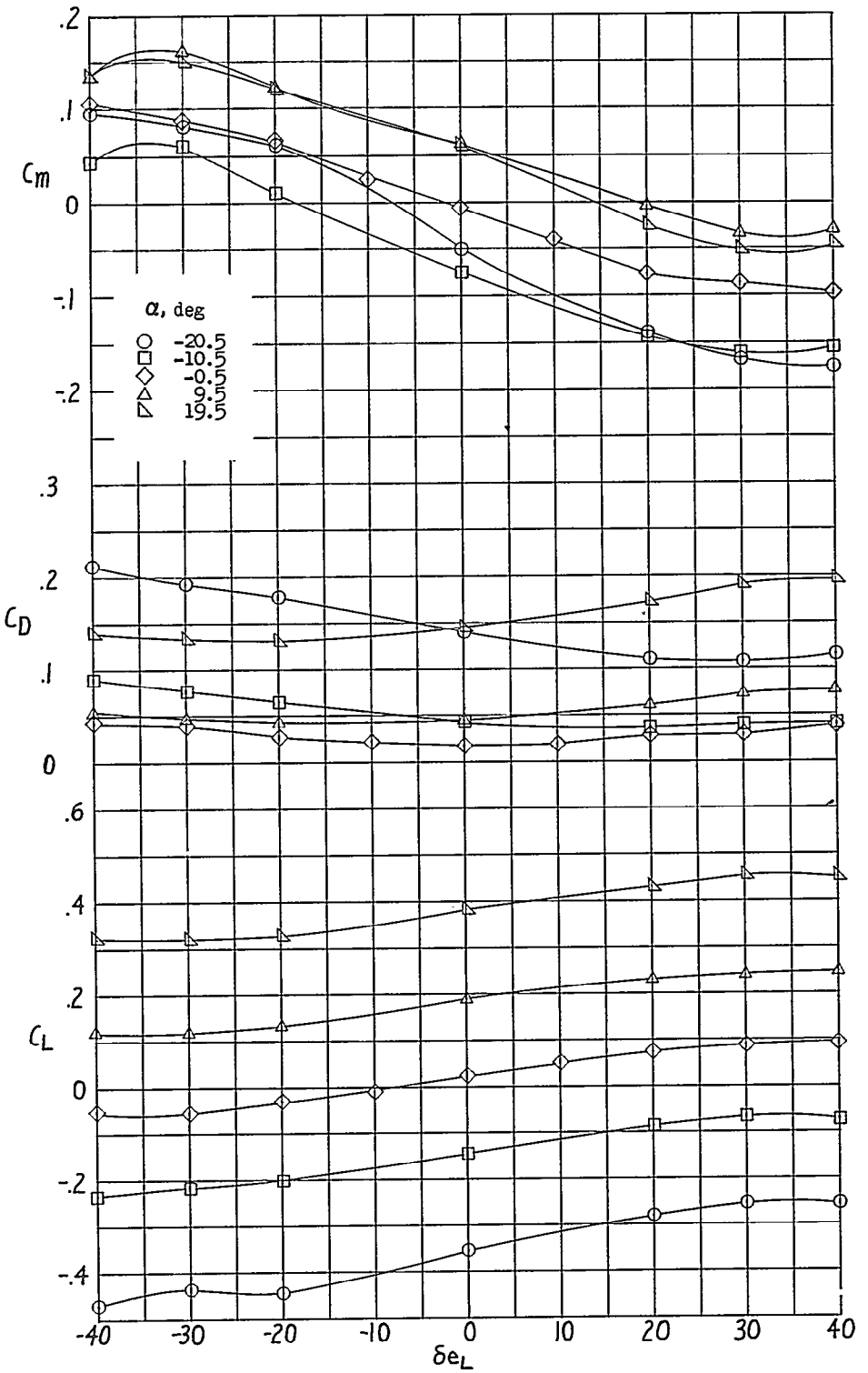

(b) $\psi = 9^\circ$.

Figure 7.- Continued.

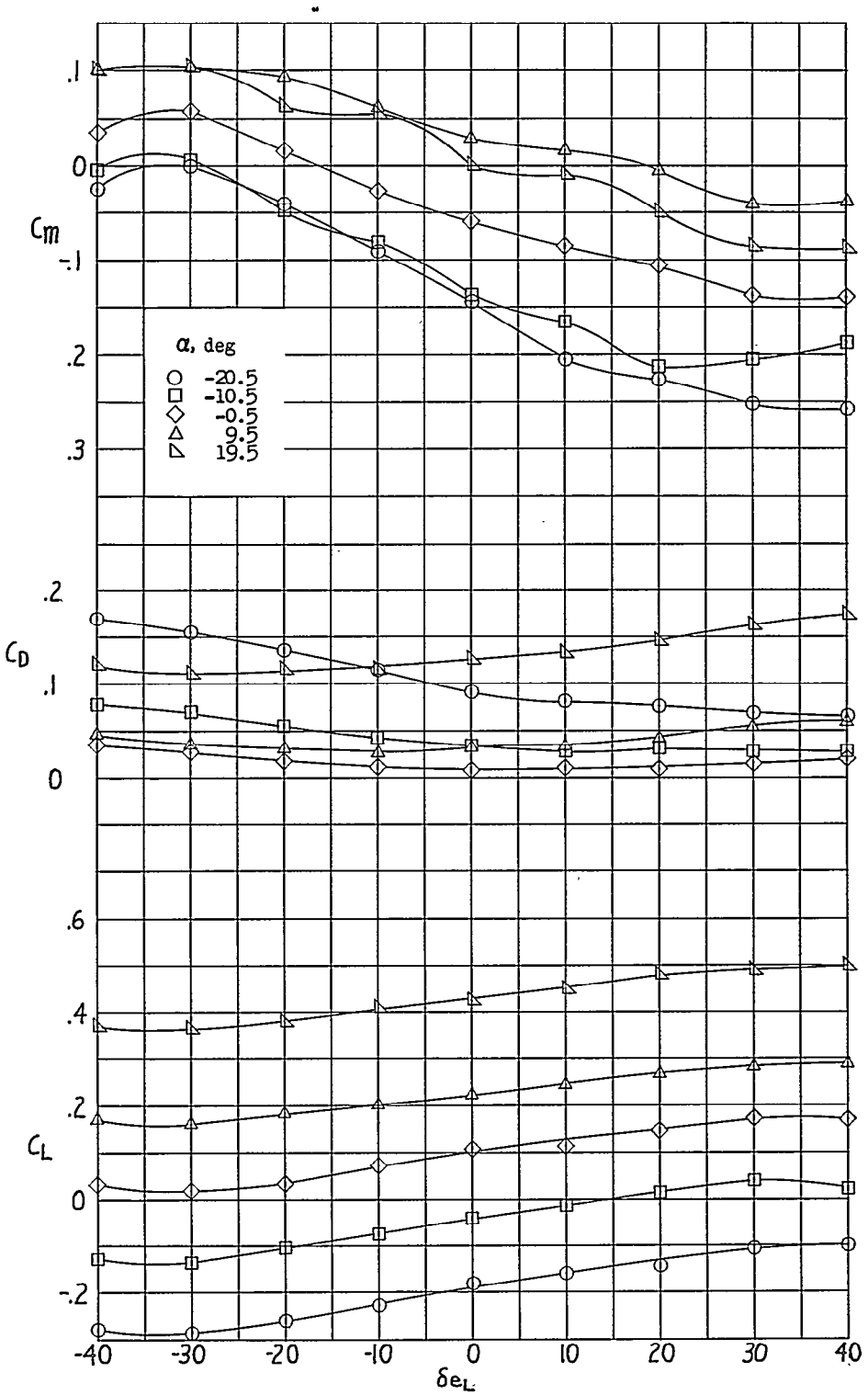

(c) $\psi = 21^\circ$.

Figure 7.- Continued.

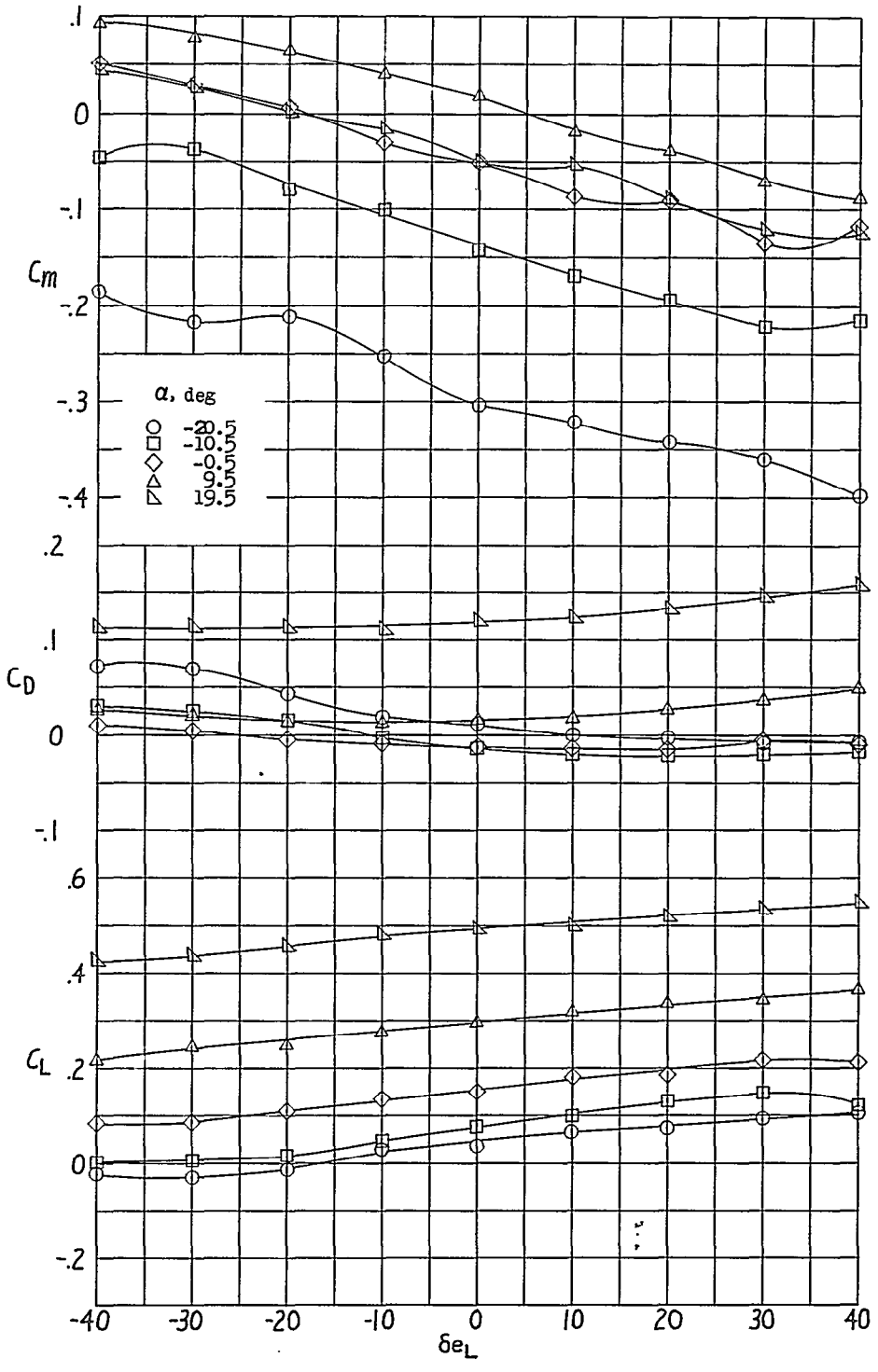

(d) $\psi = 30^\circ$.

Figure 7.- Concluded.

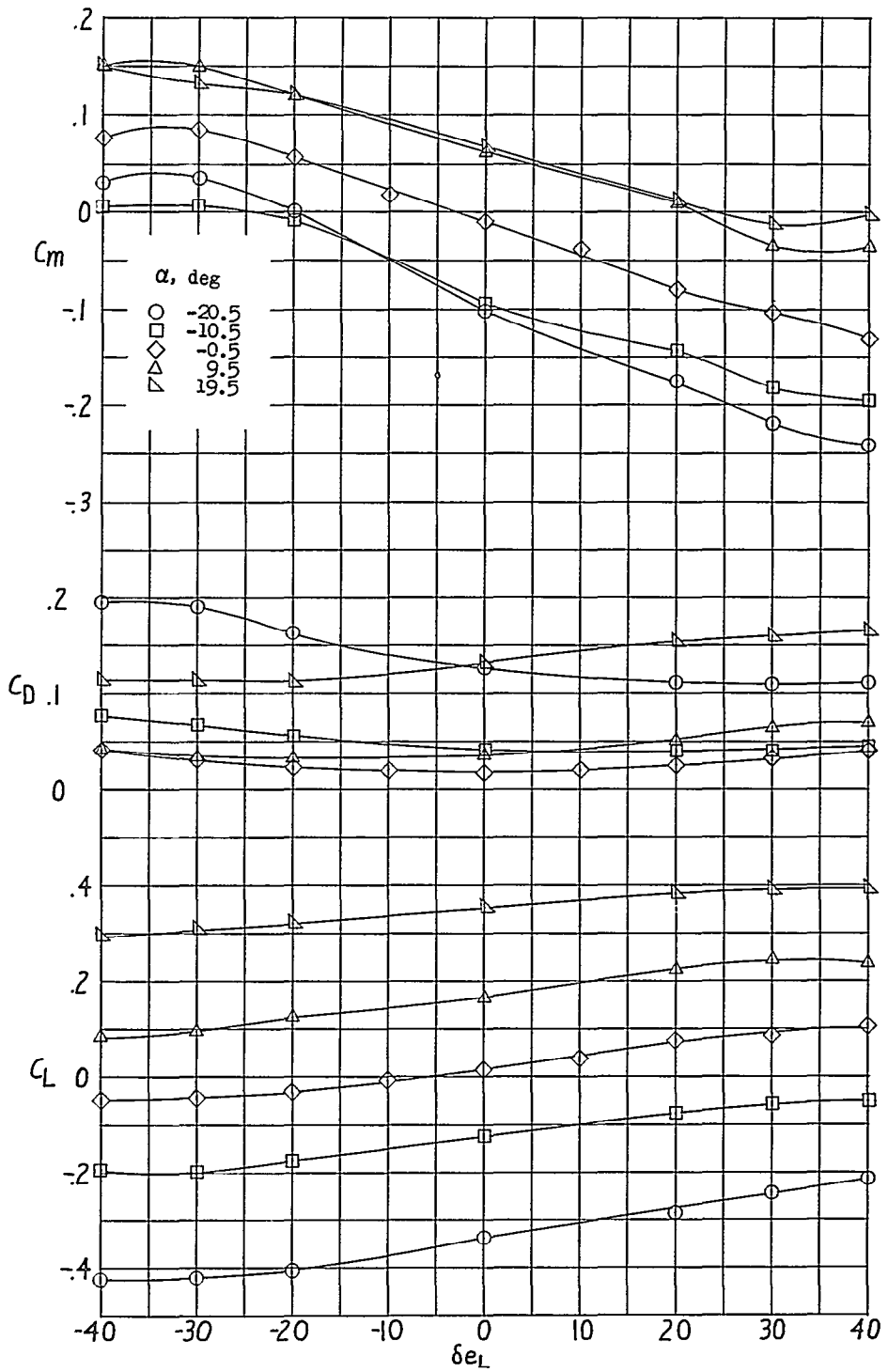

(a) $\psi = 0^o$.

Figure 8.- Effect of left elevator deflection on the longitudinal characteristics. High-aspect-ratio tail installed; $\delta_r = 0^o$; $\delta e_R = 0^o$.

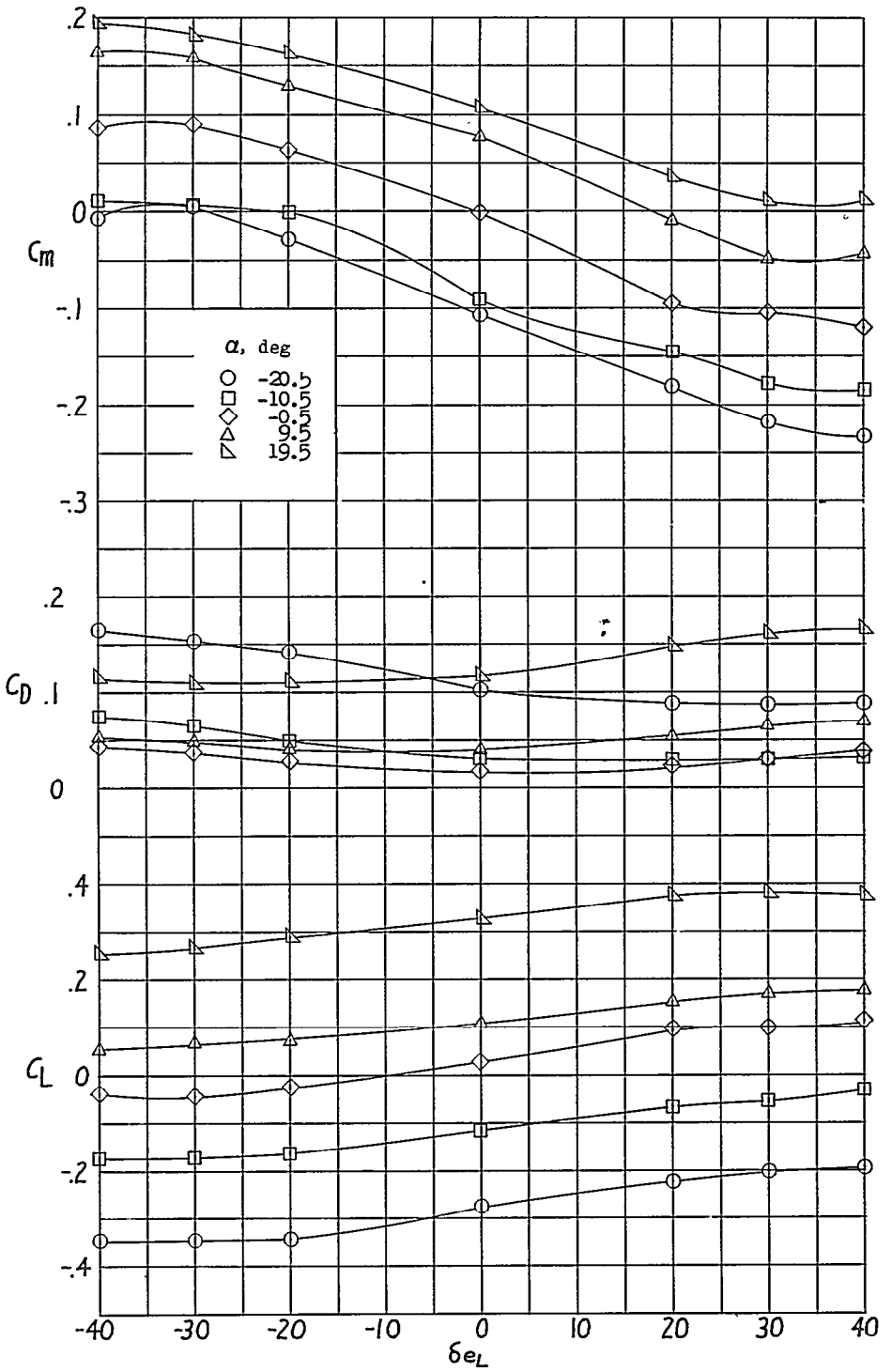

(b) $\psi = 9^{\circ}$.

Figure 8 - Continued.

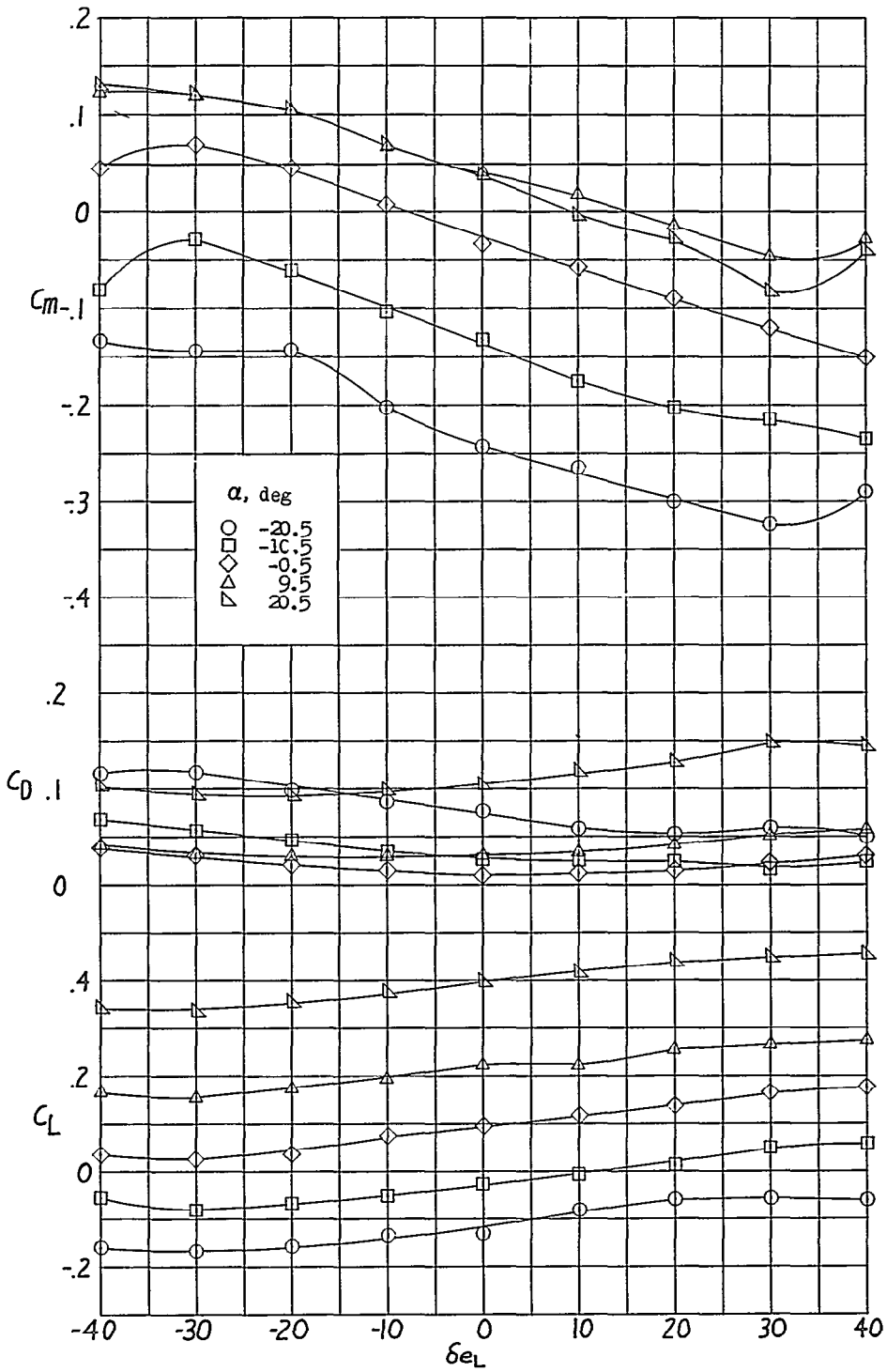

(c) $\psi = 21^\circ$.

Figure 8.- Continued.

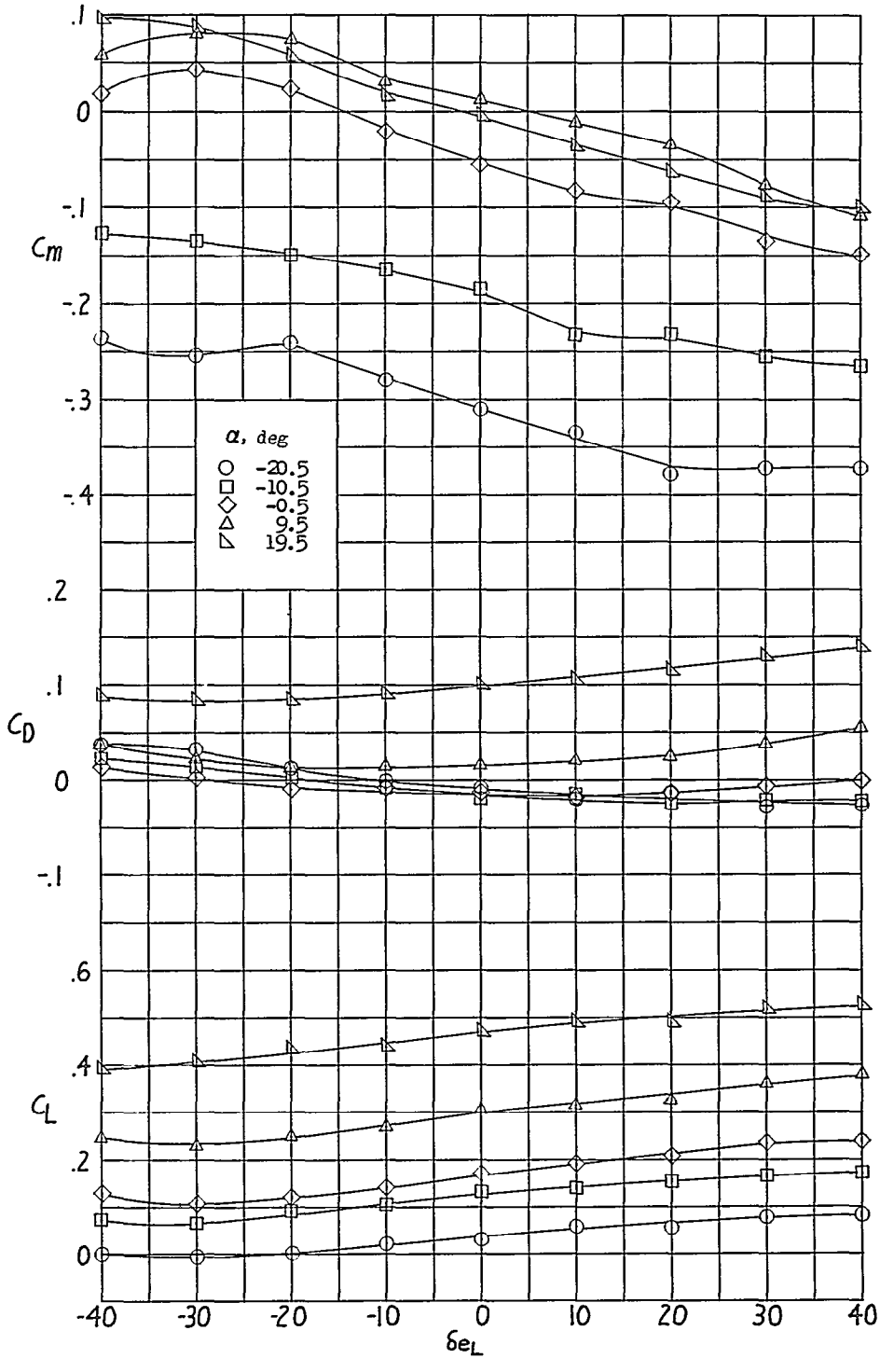

(d) $\psi = 30^{\circ}$.

Figure 8.- Concluded.

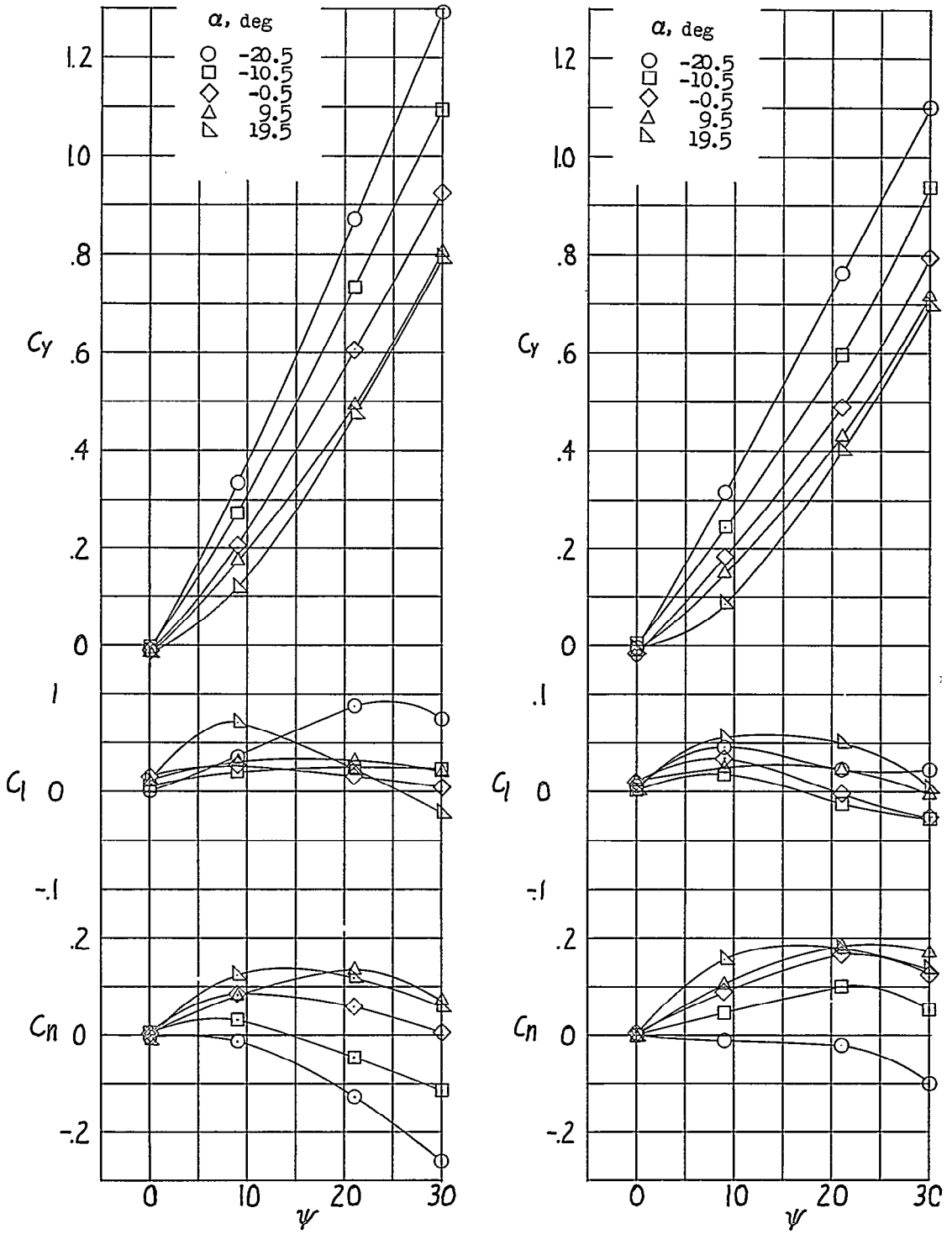

(a) Standard tail.

(b) High-aspect-ratio tail.

Figure 9.- Lateral characteristics of the Goodyear XZP5K model for two tail configurations. $\delta_r = 0^o$; $\delta_{e_L} = 0^o$; $\delta_{e_R} = 0^o$.

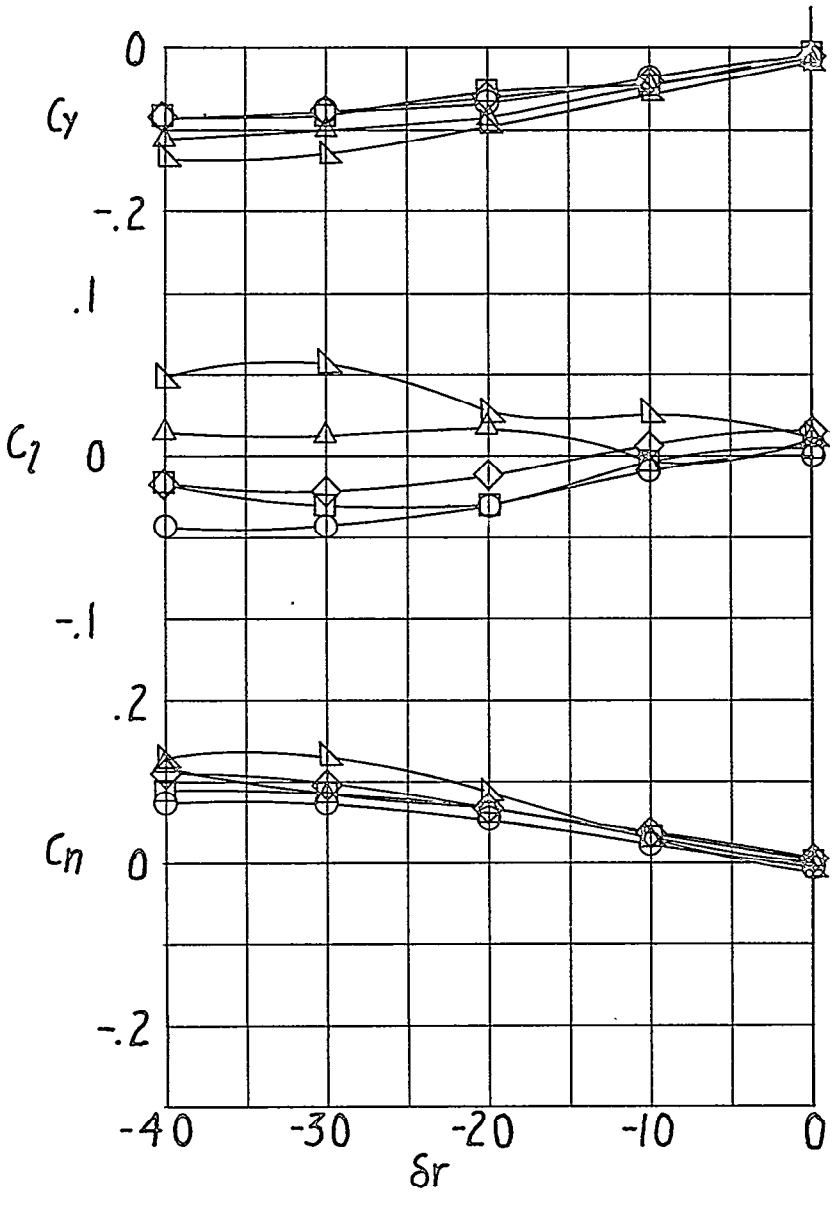

(a) $\psi = 0^{\circ}$.

Figure 10.- Effect of rudder deflection on the lateral characteristics. Standard tail installed; $\delta_{e_L} = 0^{\circ}$; $\delta_{e_R} = 0^{\circ}$.

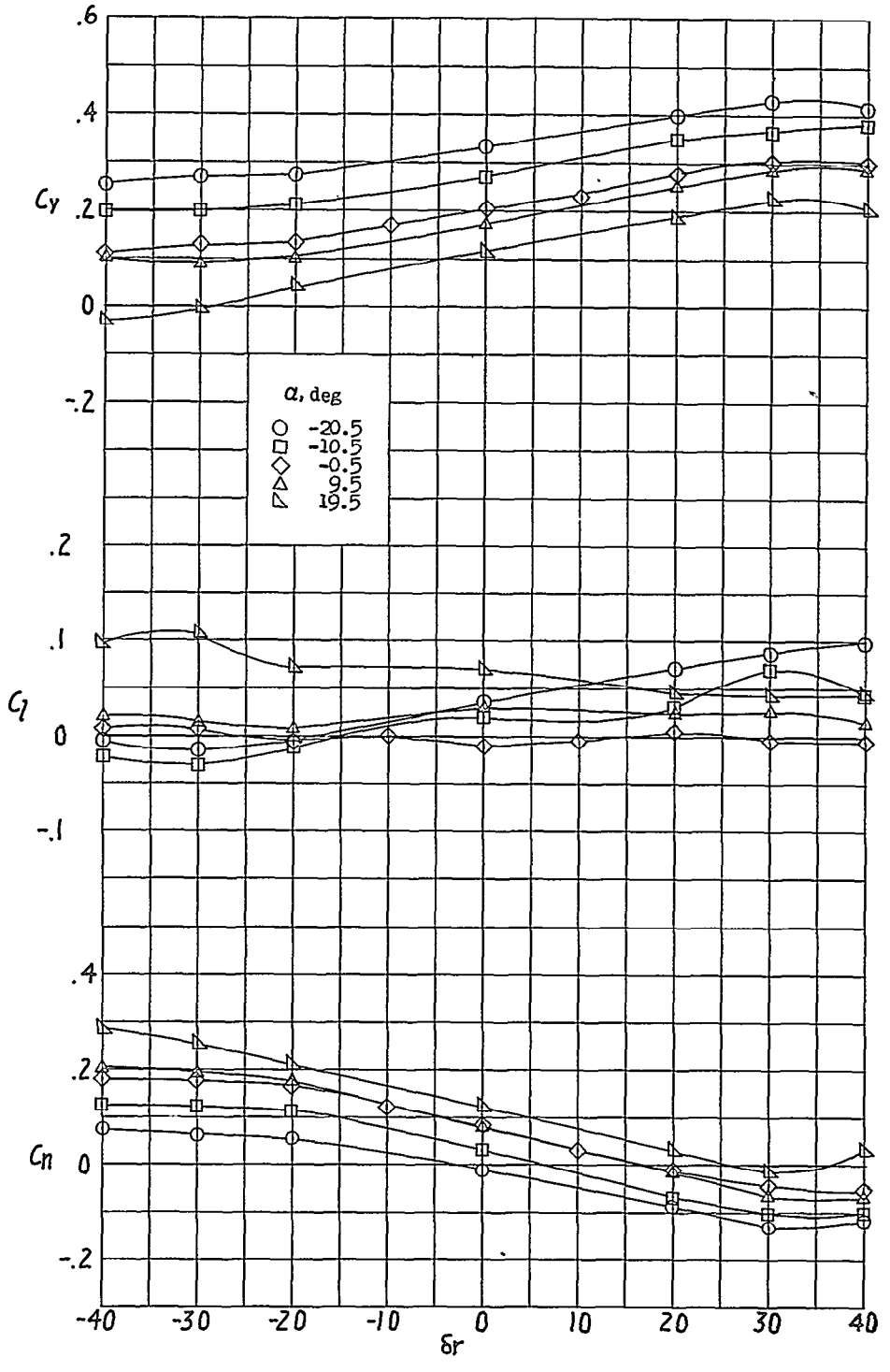

(b) $\psi = 9^{\circ}$.

Figure 10.- Continued.

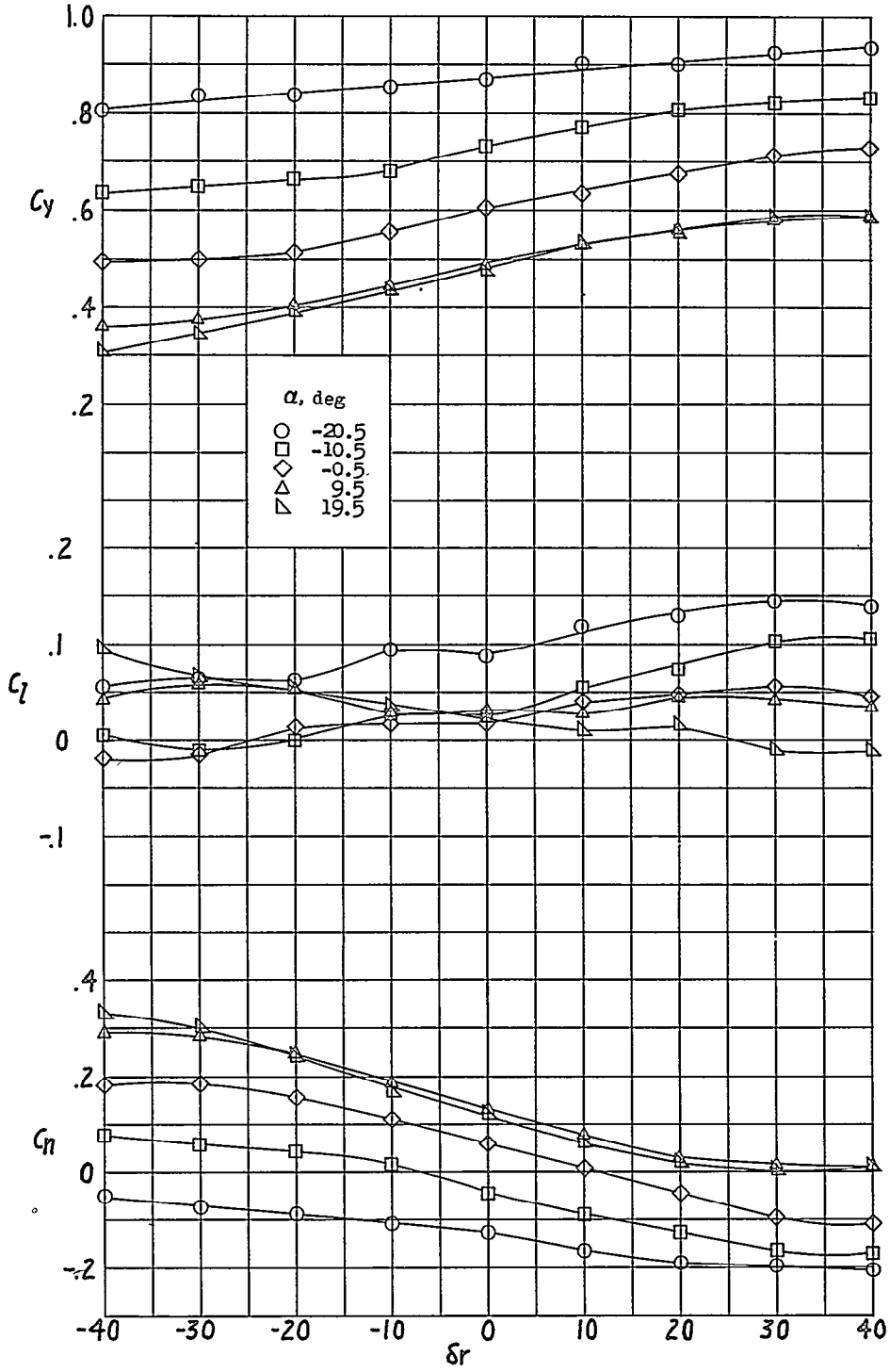

(c) $\psi = 21^{\circ}$.

Figure 10.- Continued.

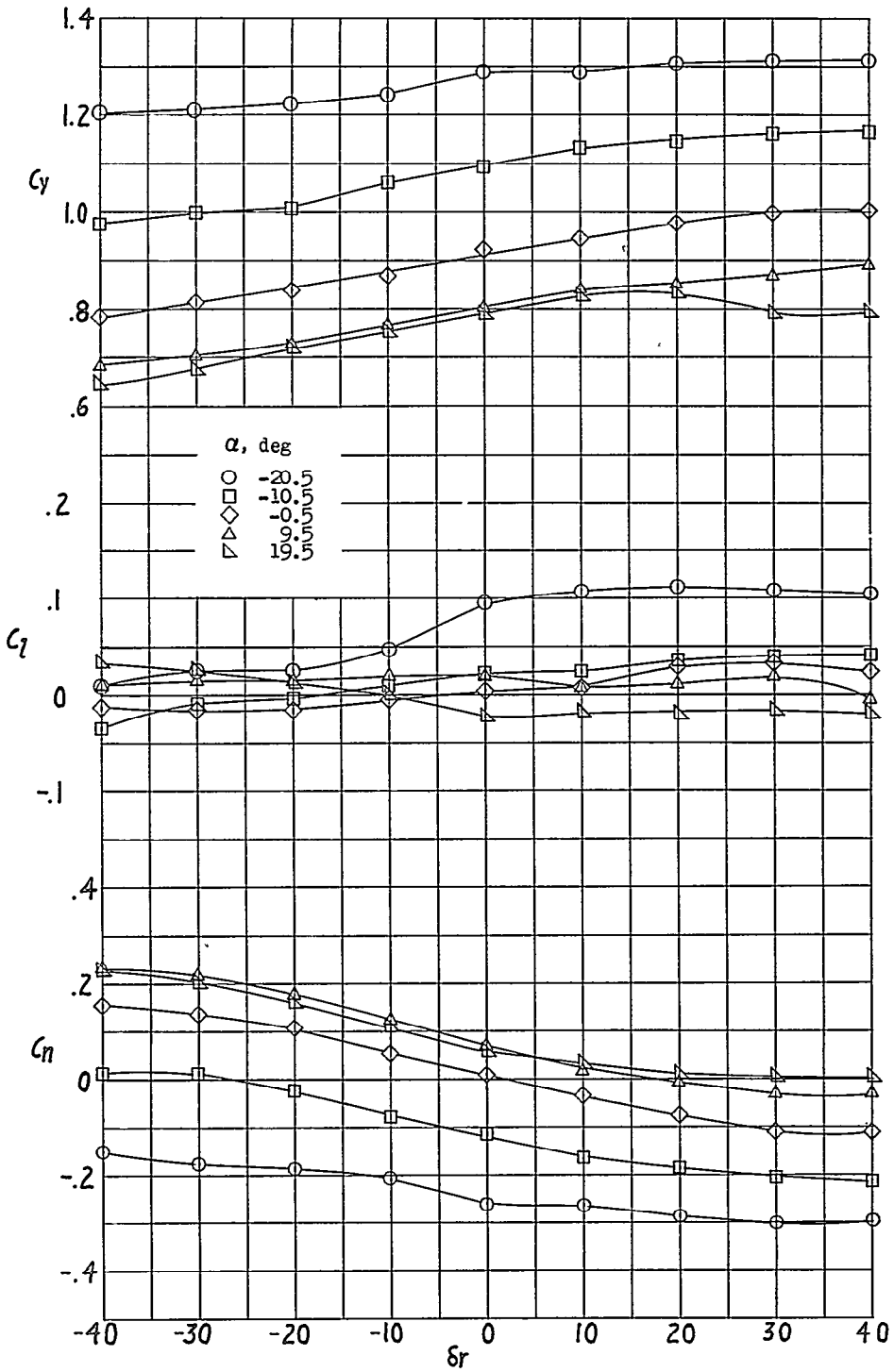

(d) $\psi = 30^\circ$.

Figure 10.- Concluded.

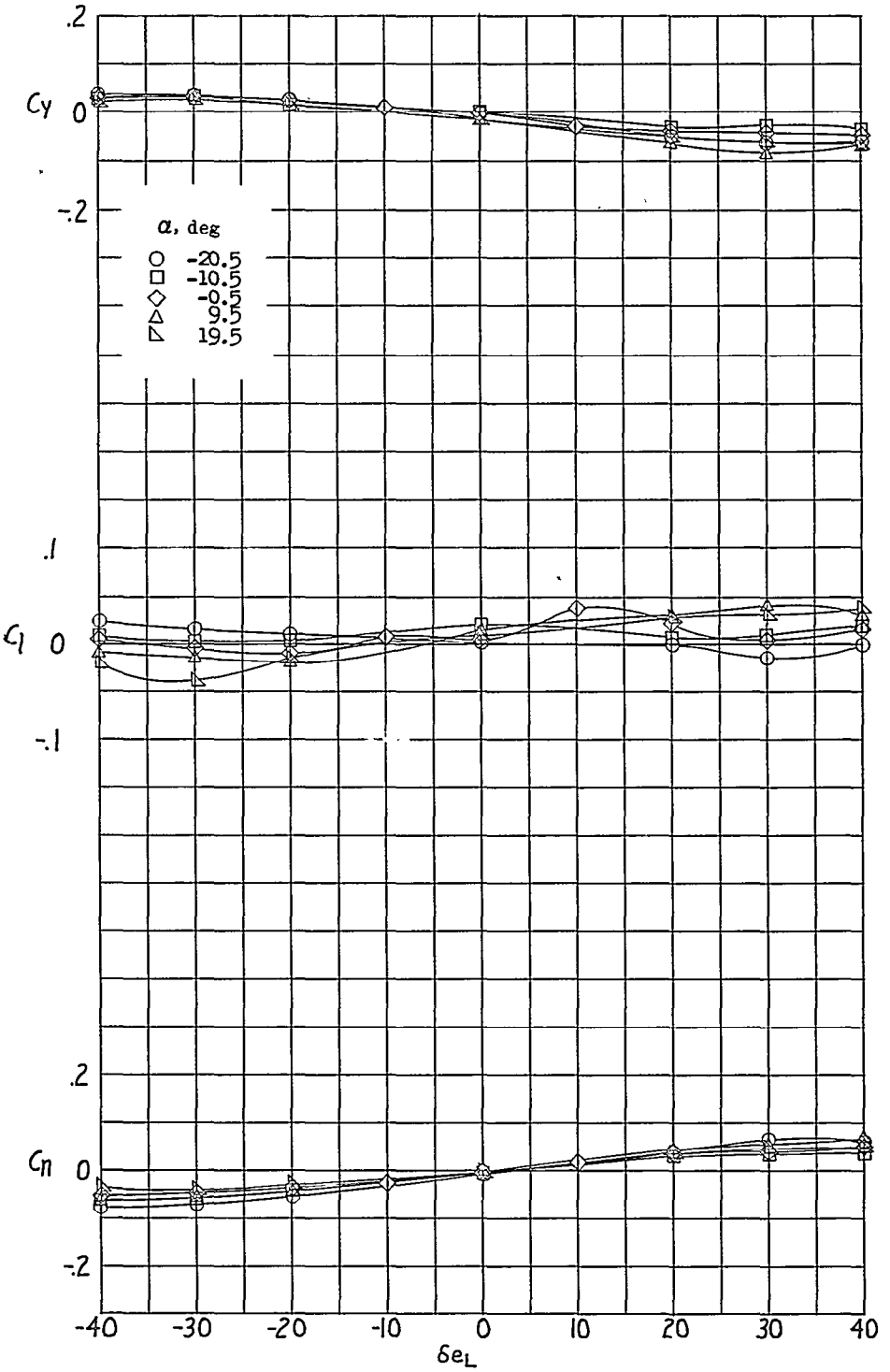

(a) $\psi = 0^\circ$.

Figure 11.- Effect of left elevator deflection on the lateral characteristics. Standard tail installed; $\delta_{e_R} = 0^\circ$; $\delta_r = 0^\circ$.

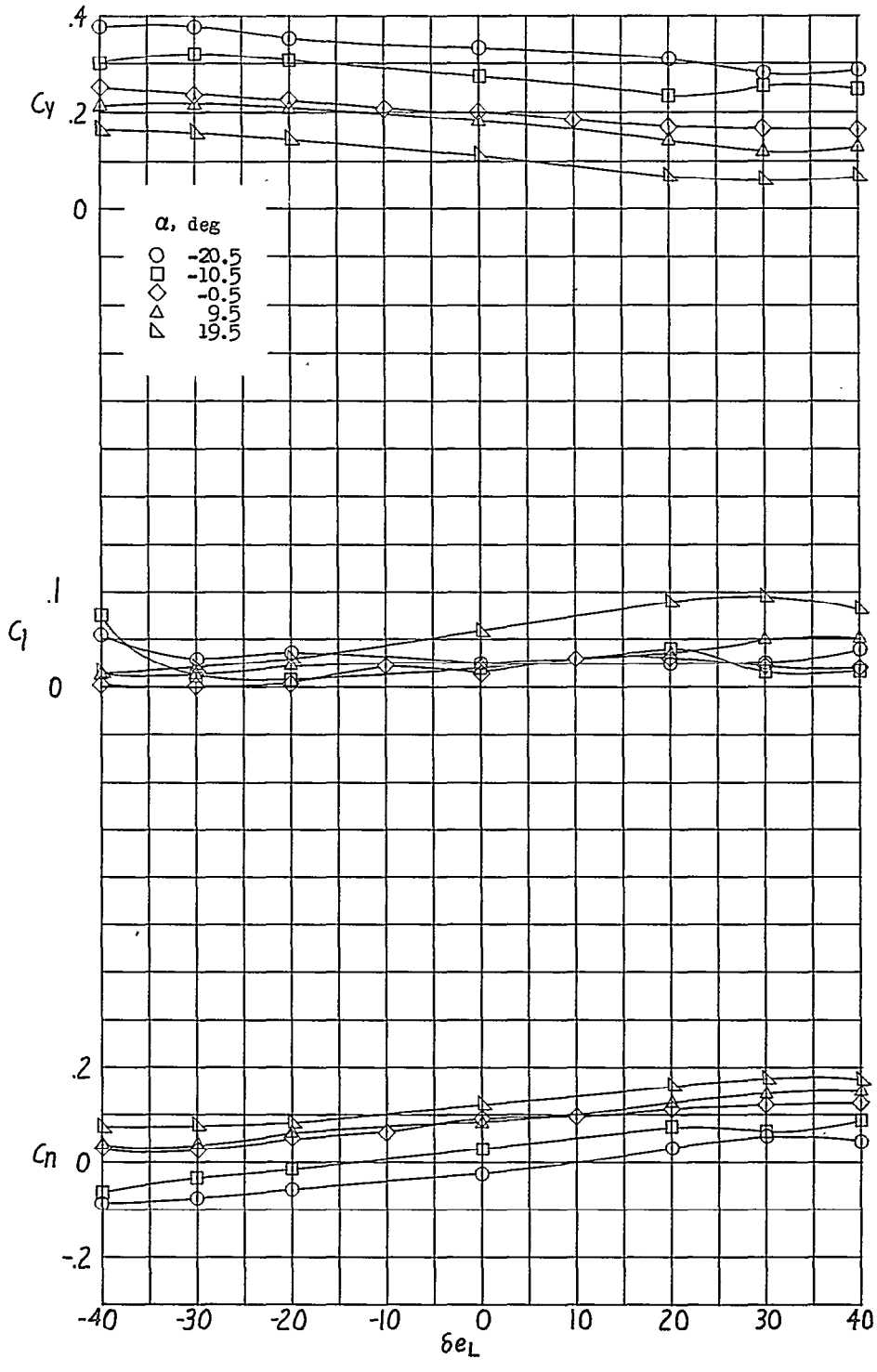

(b) $\psi = 9^{\circ}$.

Figure 11.- Continued.

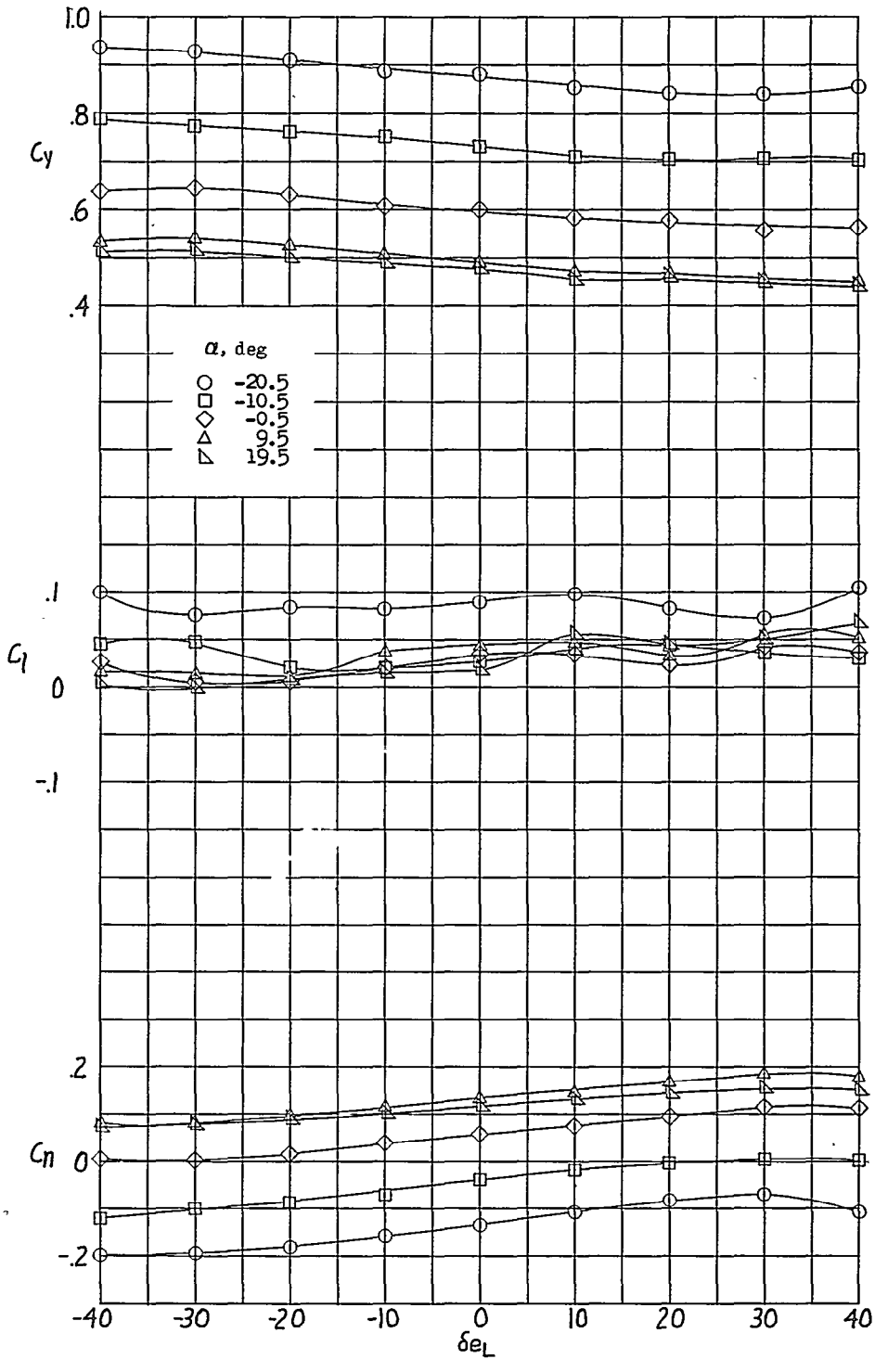

(c) $\psi = 21^\circ$.

Figure 11.- Continued.

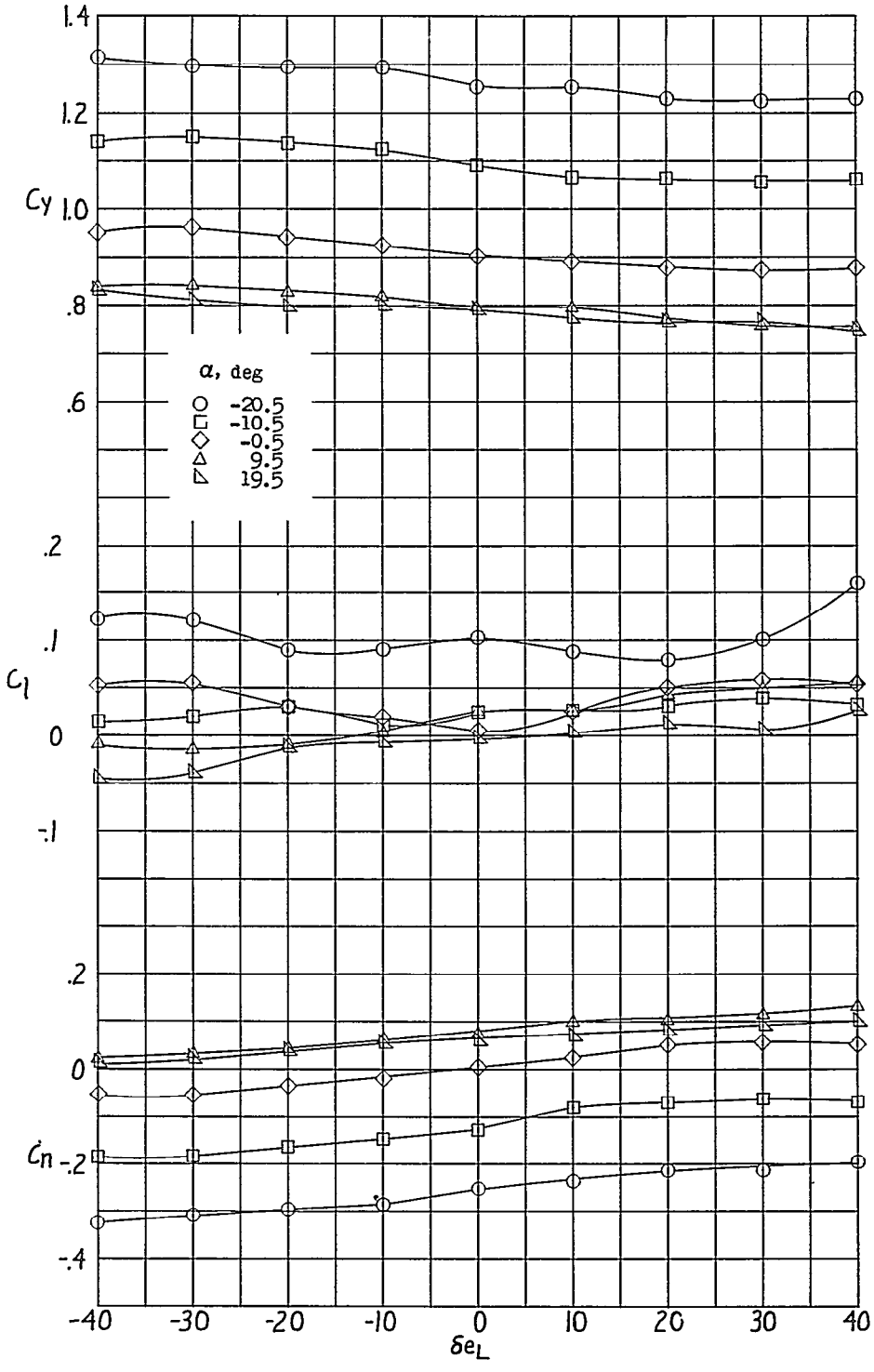

(d) $\psi = 30^\circ$.

Figure 11.- Concluded.

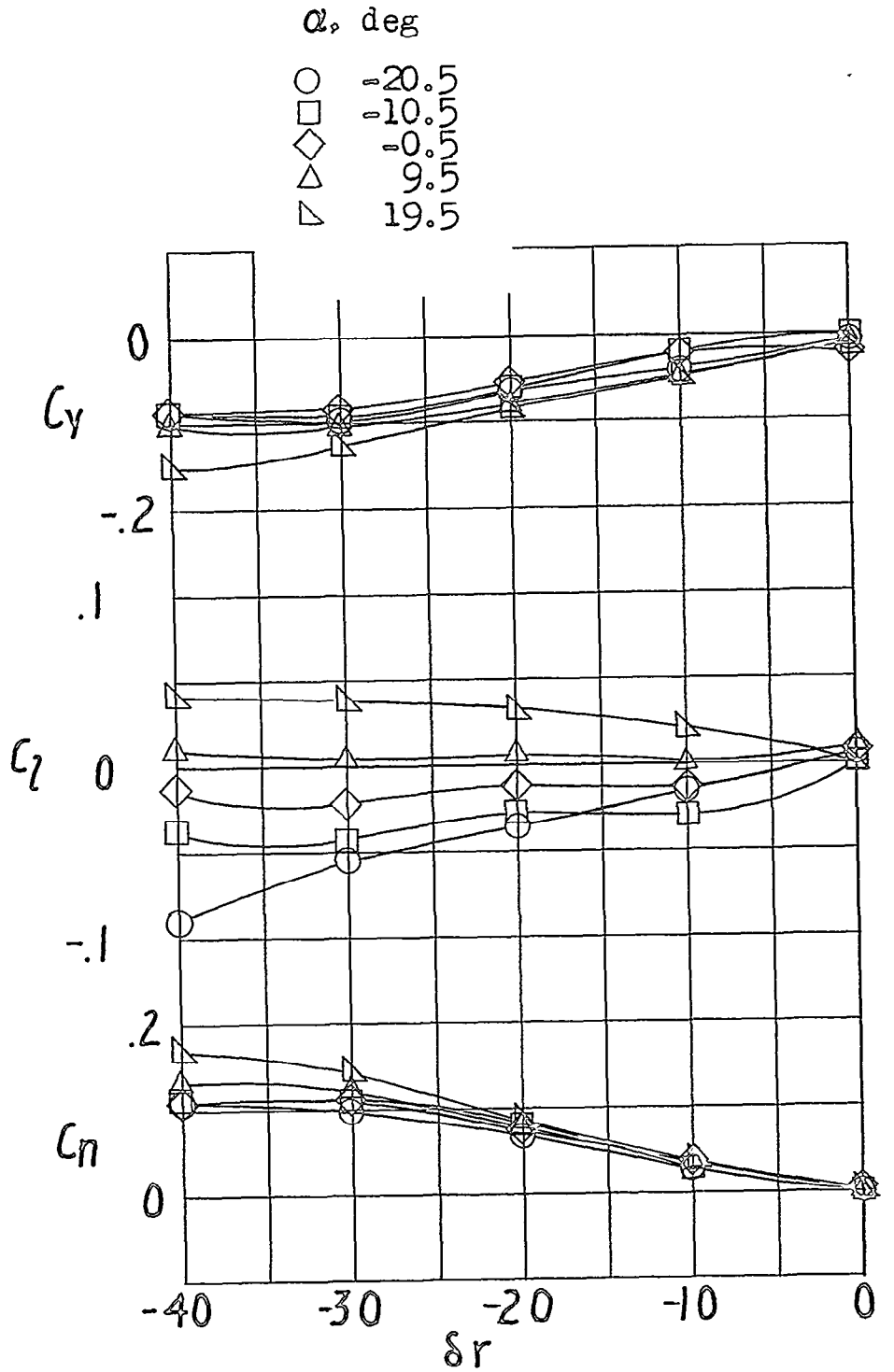

(a) $\psi = 0^{\circ}$.

Figure 12.- Effect of rudder deflection on the lateral characteristics. High-aspect-ratio tail installed; $\delta_{e_L} = 0^{\circ}$; $\delta_{e_R} = 0^{\circ}$.

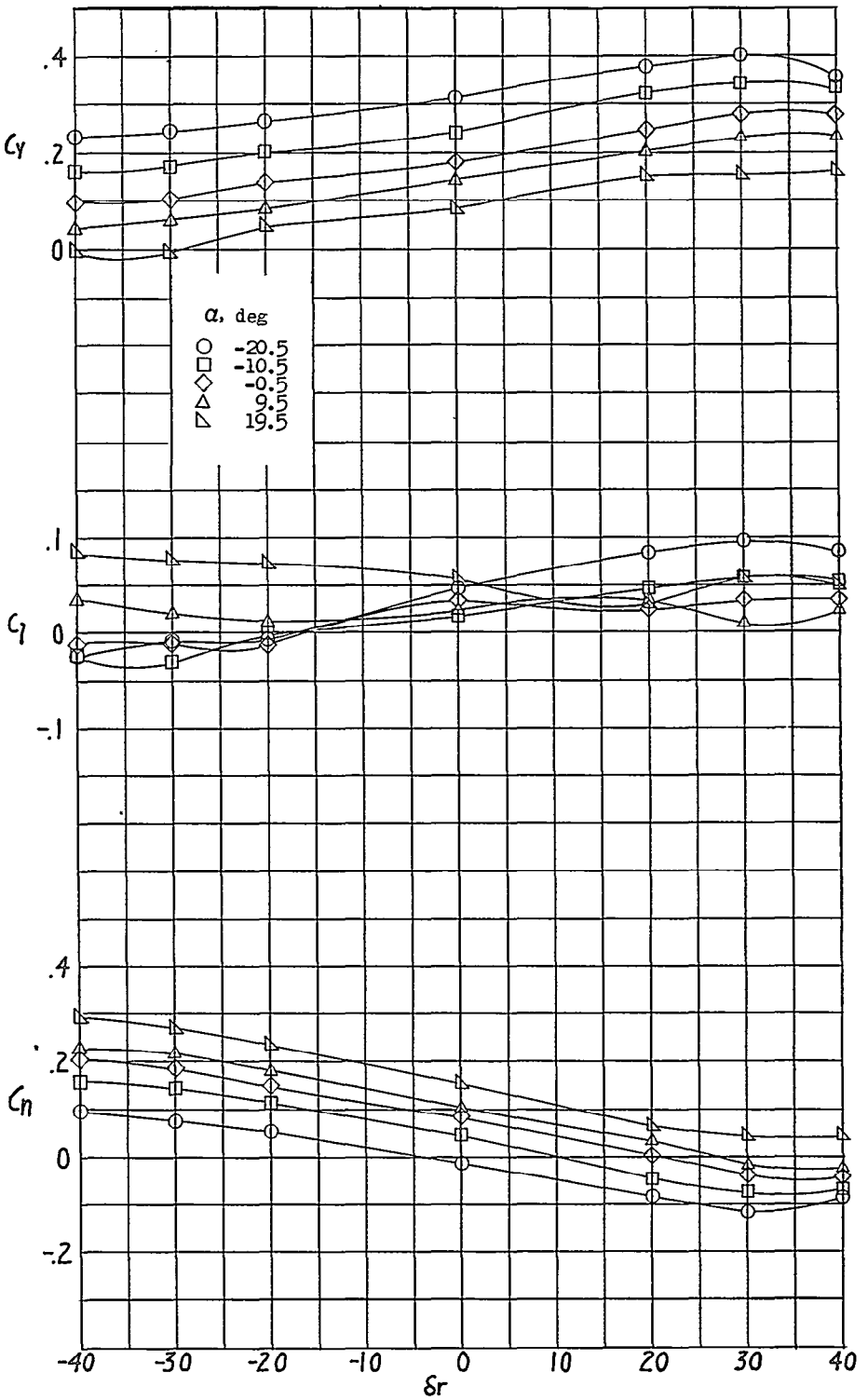

(b) $\psi = 9^{\circ}$.

Figure 12.- Continued.

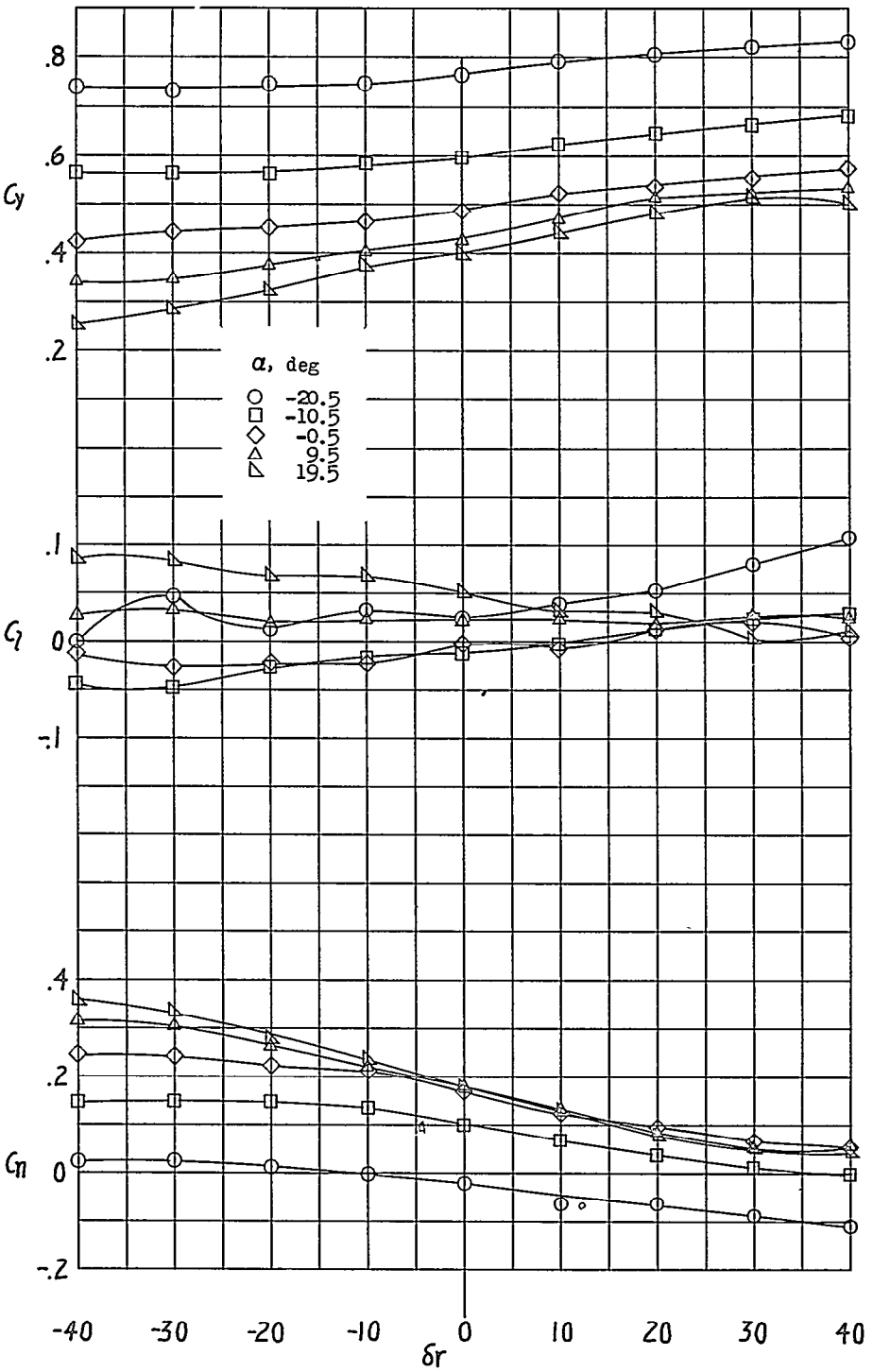

(c) $\psi = 21^{\circ}$.

Figure 12.- Continued.

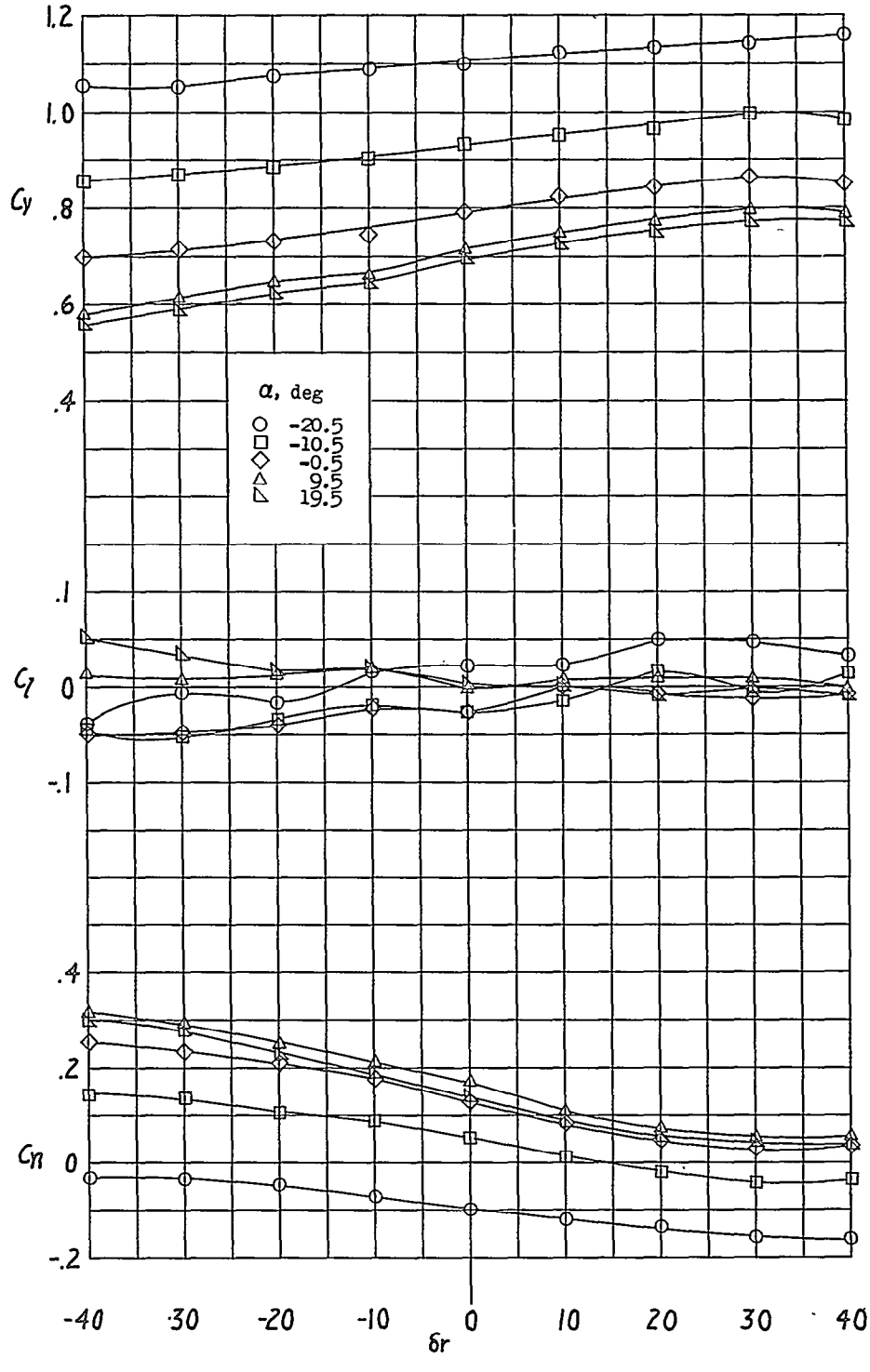

(d) $\psi = 30^{\circ}$.

Figure 12.- Concluded.

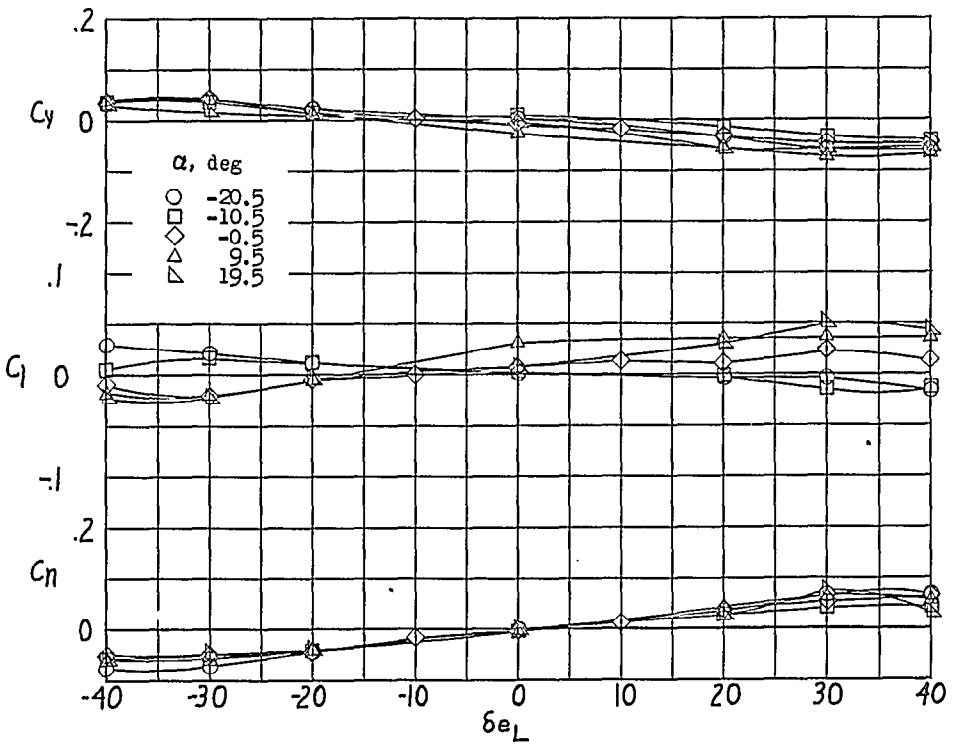

(a) $\psi = 0^\circ$.

Figure 13.- Effect of left elevator deflection on the lateral characteristics. High-aspect-ratio tail installed; $\delta_r = 0^\circ$; $\delta_{e_R} = 0^\circ$.

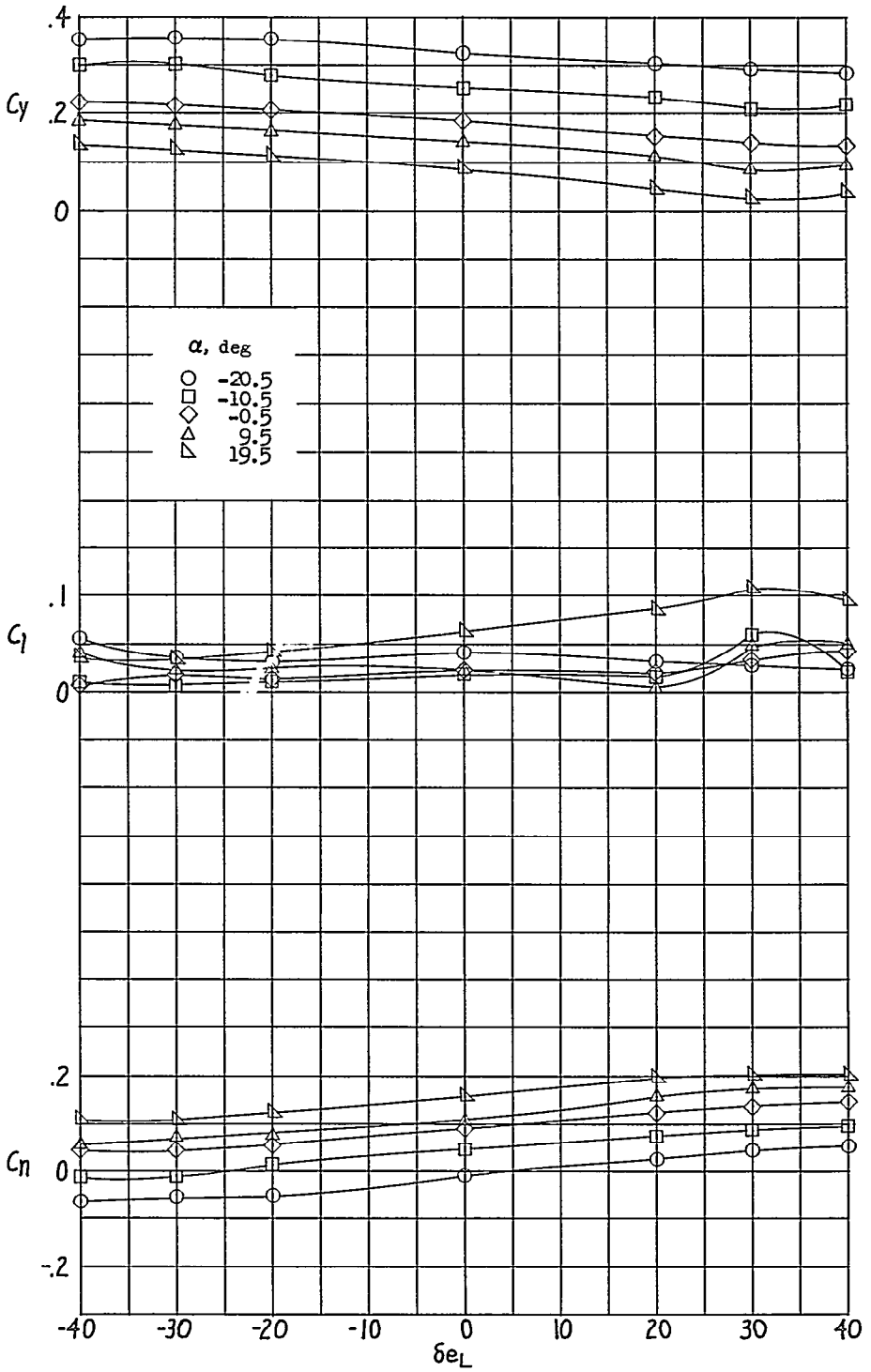

(b) $\psi = 9^{\circ}$.

Figure 13.- Continued.

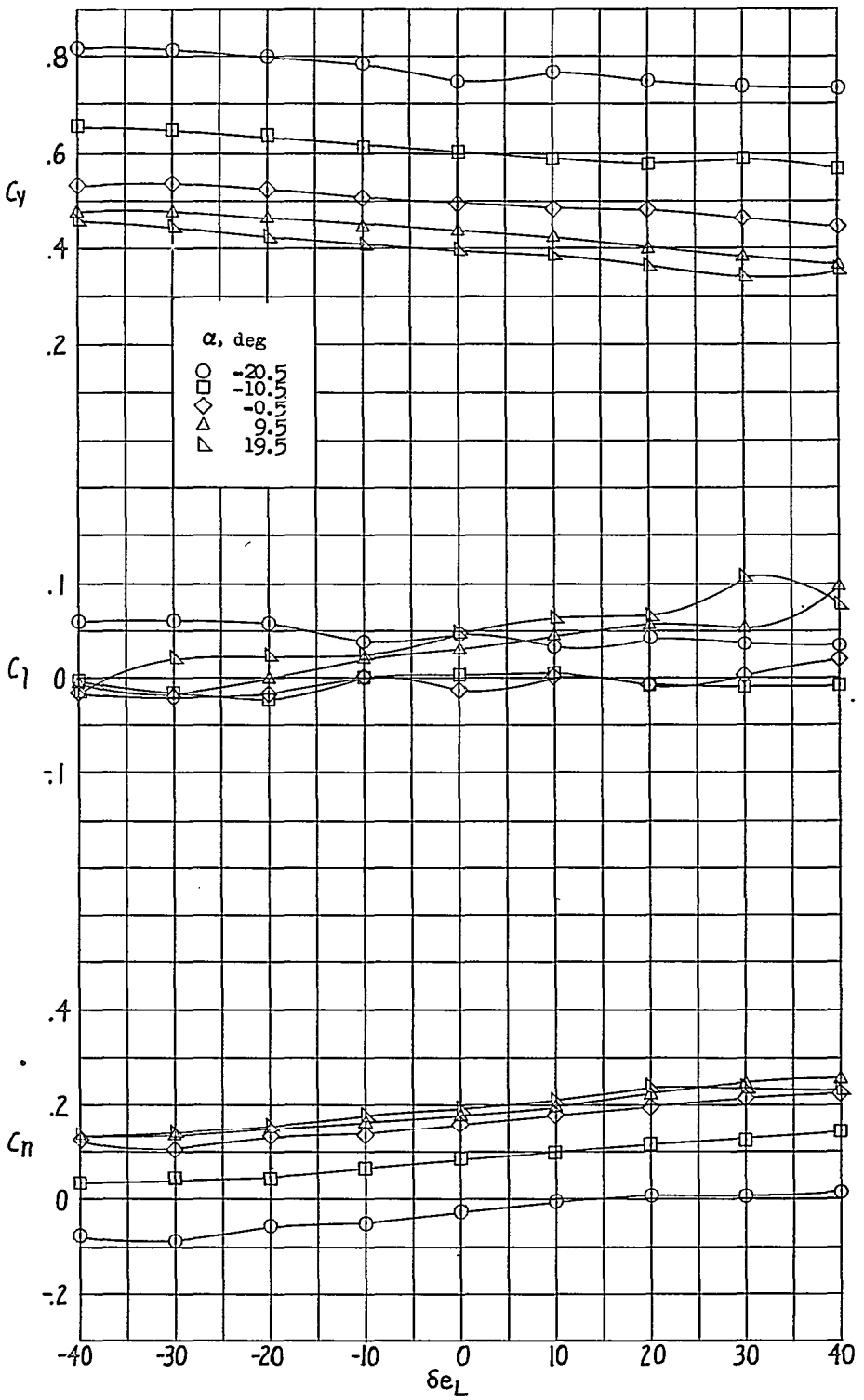

(c) $\psi = 21^\circ$.

Figure 13.- Continued.

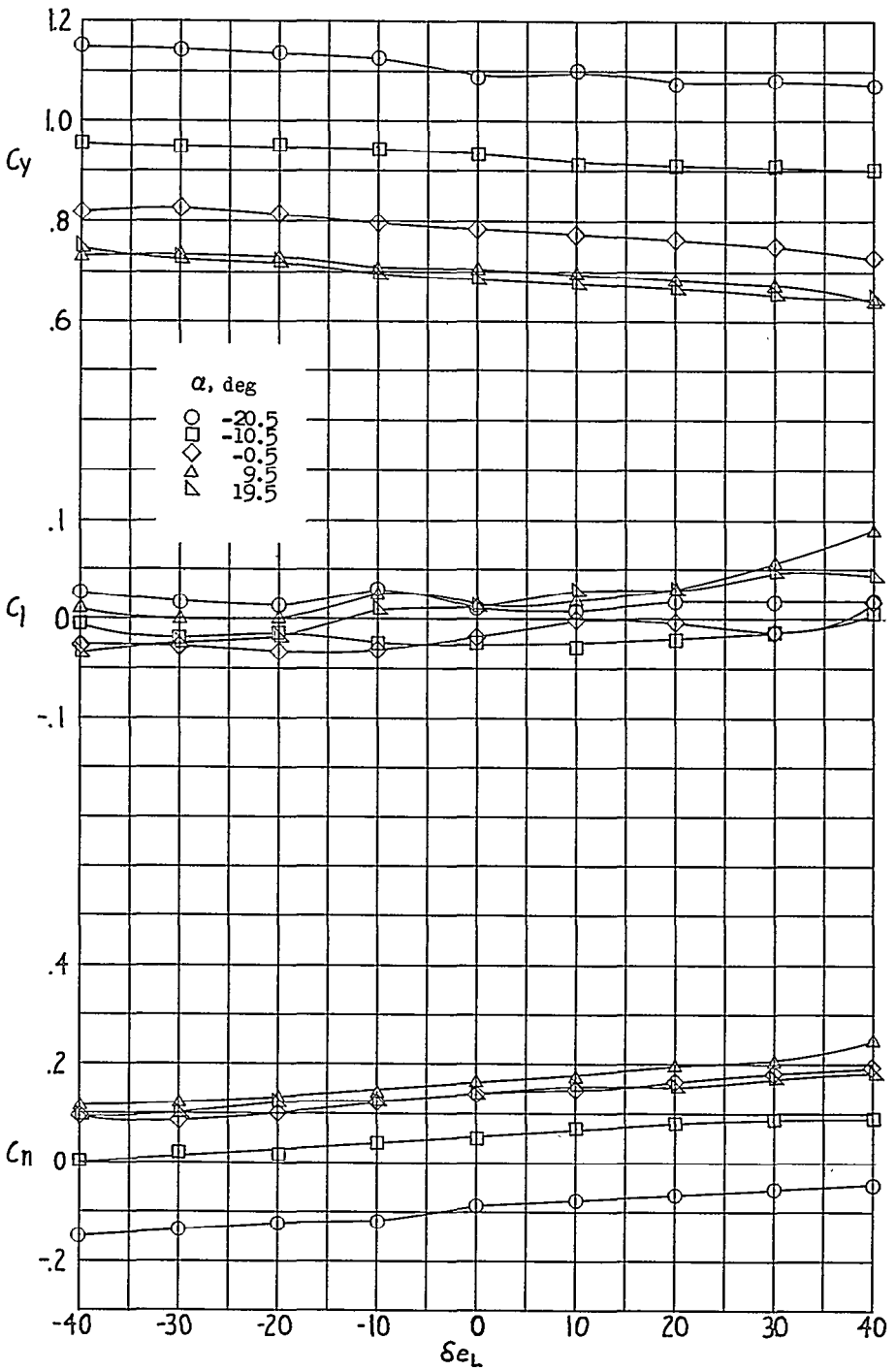

(d) $\psi = 30^\circ$.

Figure 13.- Concluded.

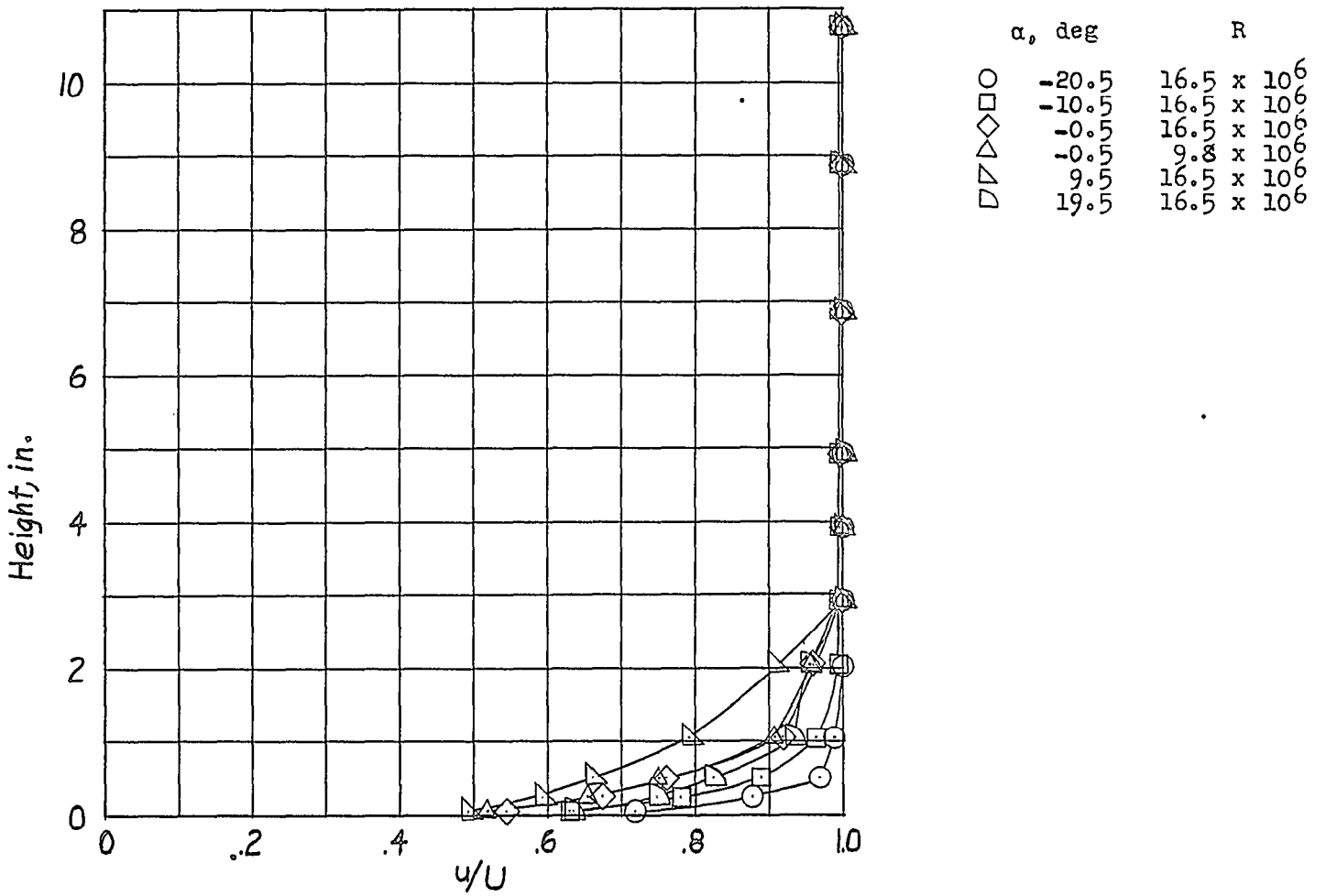

(a) Top center line. Position 0.60ℓ.

Figure 14.- Effect of angle-of-attack on velocity profiles in the boundary layer along the hull. $\psi = 0^{\circ}$; $\delta_r = 0^{\circ}$; $\delta_{e_L} = 0^{\circ}$; $\delta_{e_R} = 0^{\circ}$.

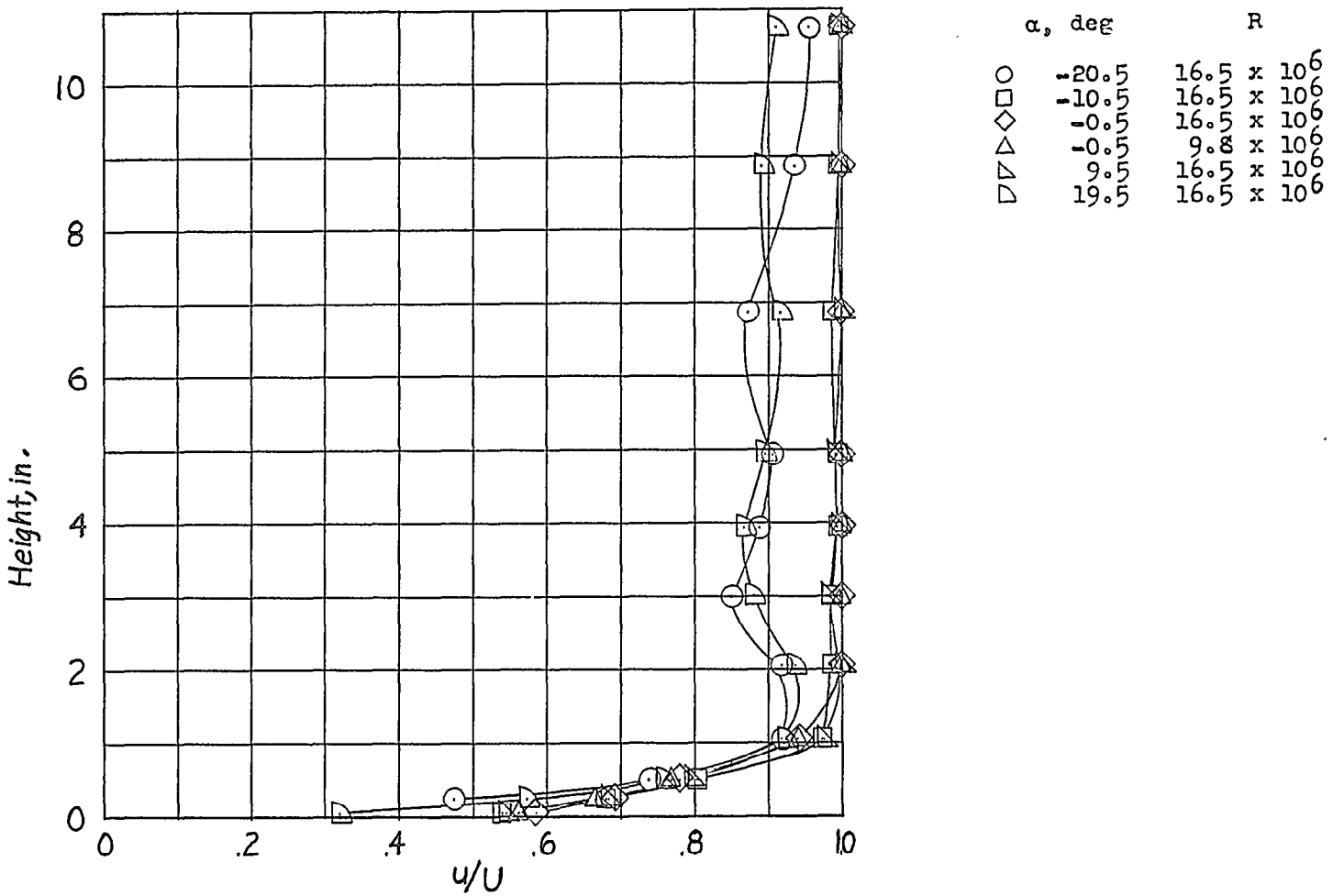

(b) Side center line. Position 0.607.

Figure 14.- Continued.

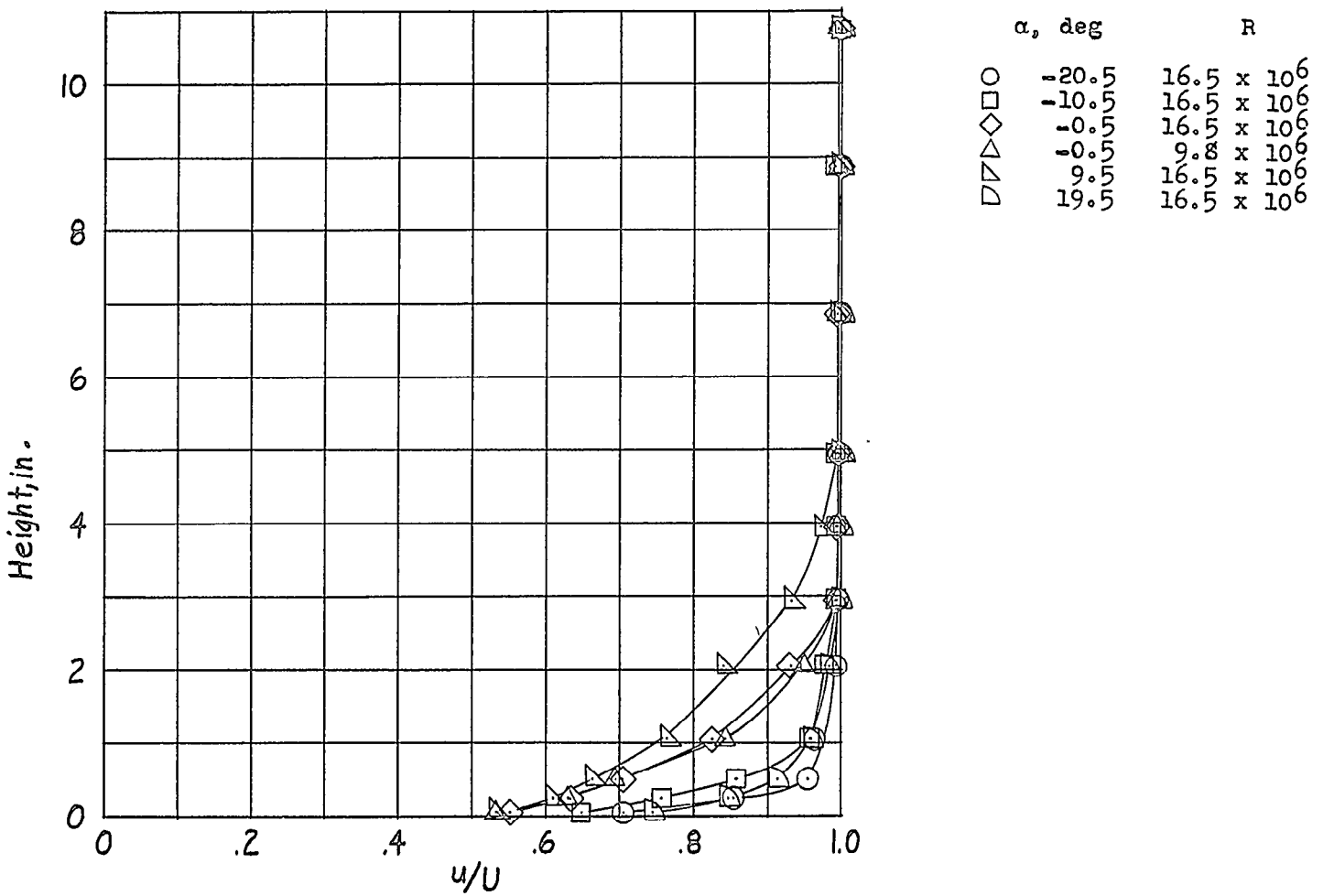

(c) Top center line. Position 0.75ℓ.

Figure 14.- Continued.

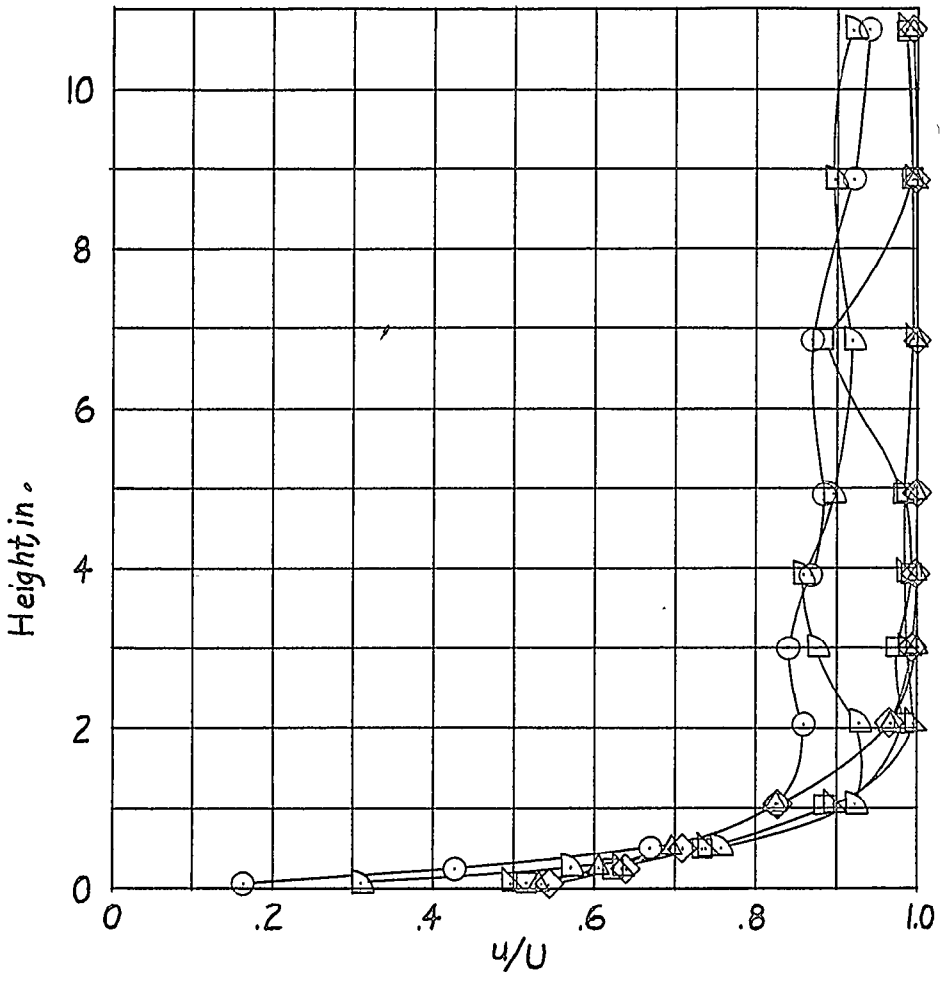

	α, deg	R
○	-20.5	16.5 × 10⁶
□	-10.5	16.5 × 10⁶
◇	-0.5	16.5 × 10⁶
◁	-0.5	9.8 × 10⁶
△	9.5	16.5 × 10⁶
▱	19.5	16.5 × 10⁶

(d) Side center line. Position 0.752.

Figure 14.- Continued.

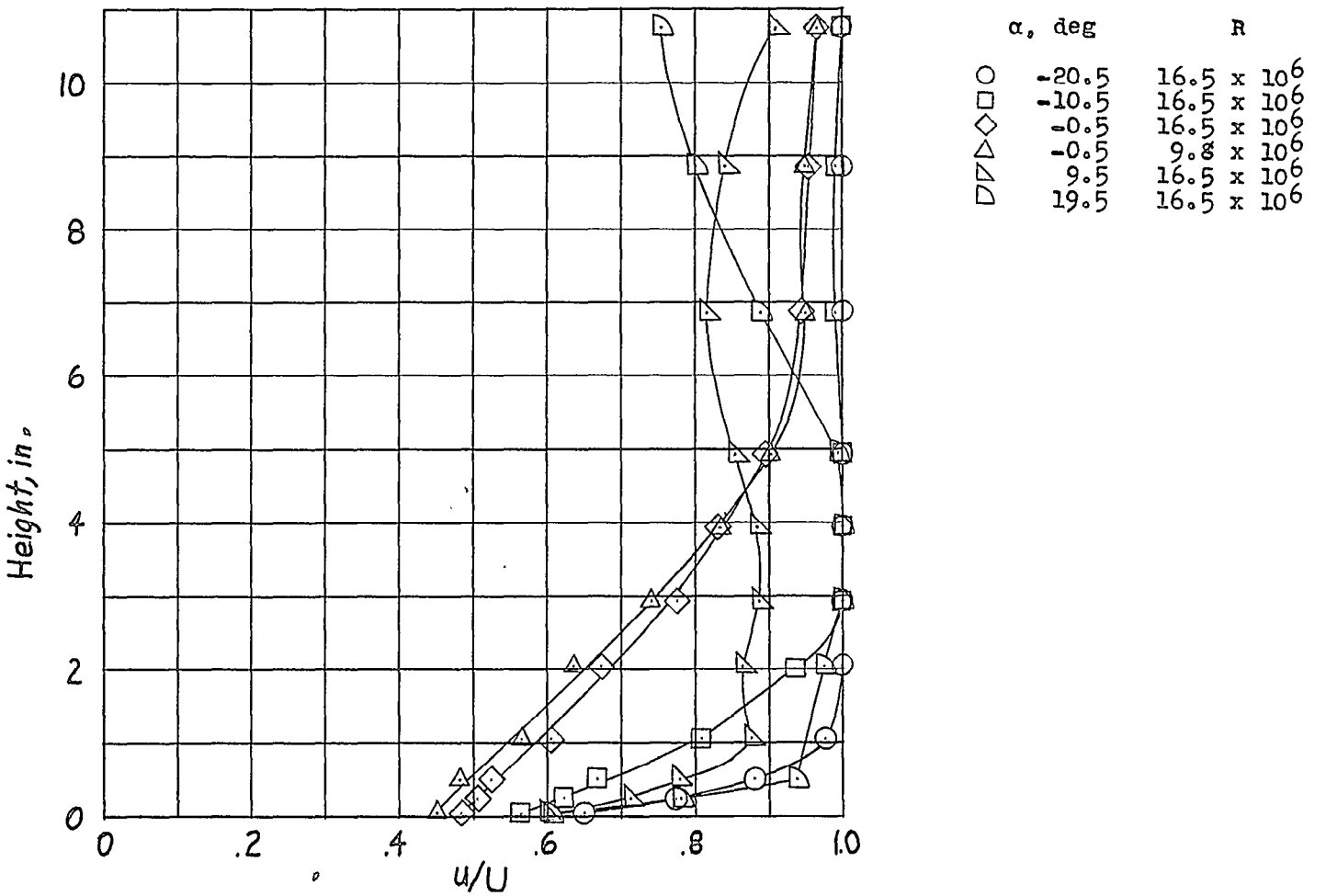

(e) Top center line. Position 0.97ℓ.

Figure 14.- Continued.

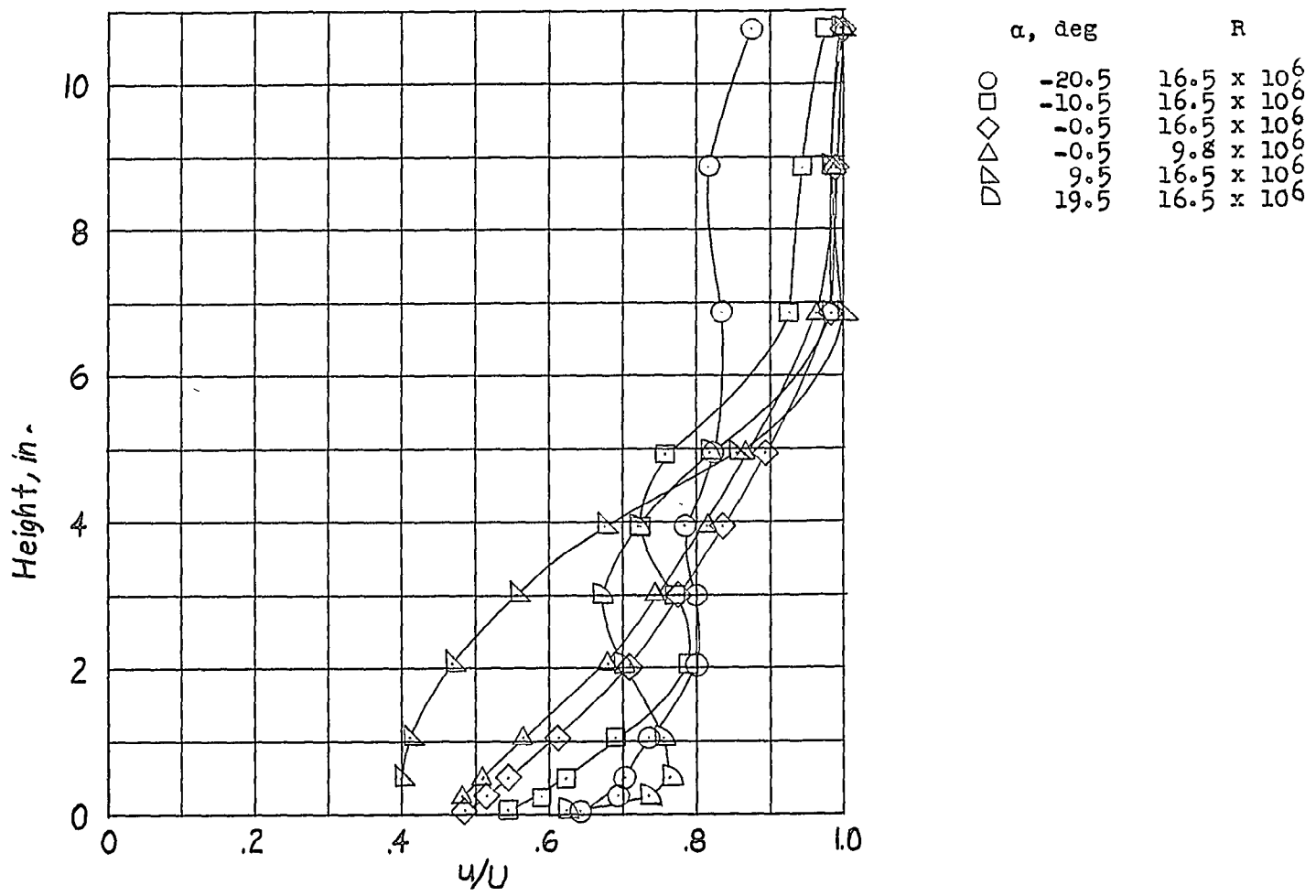

(f) Side center line. Position 0.97ℓ.

Figure 14.- Concluded.

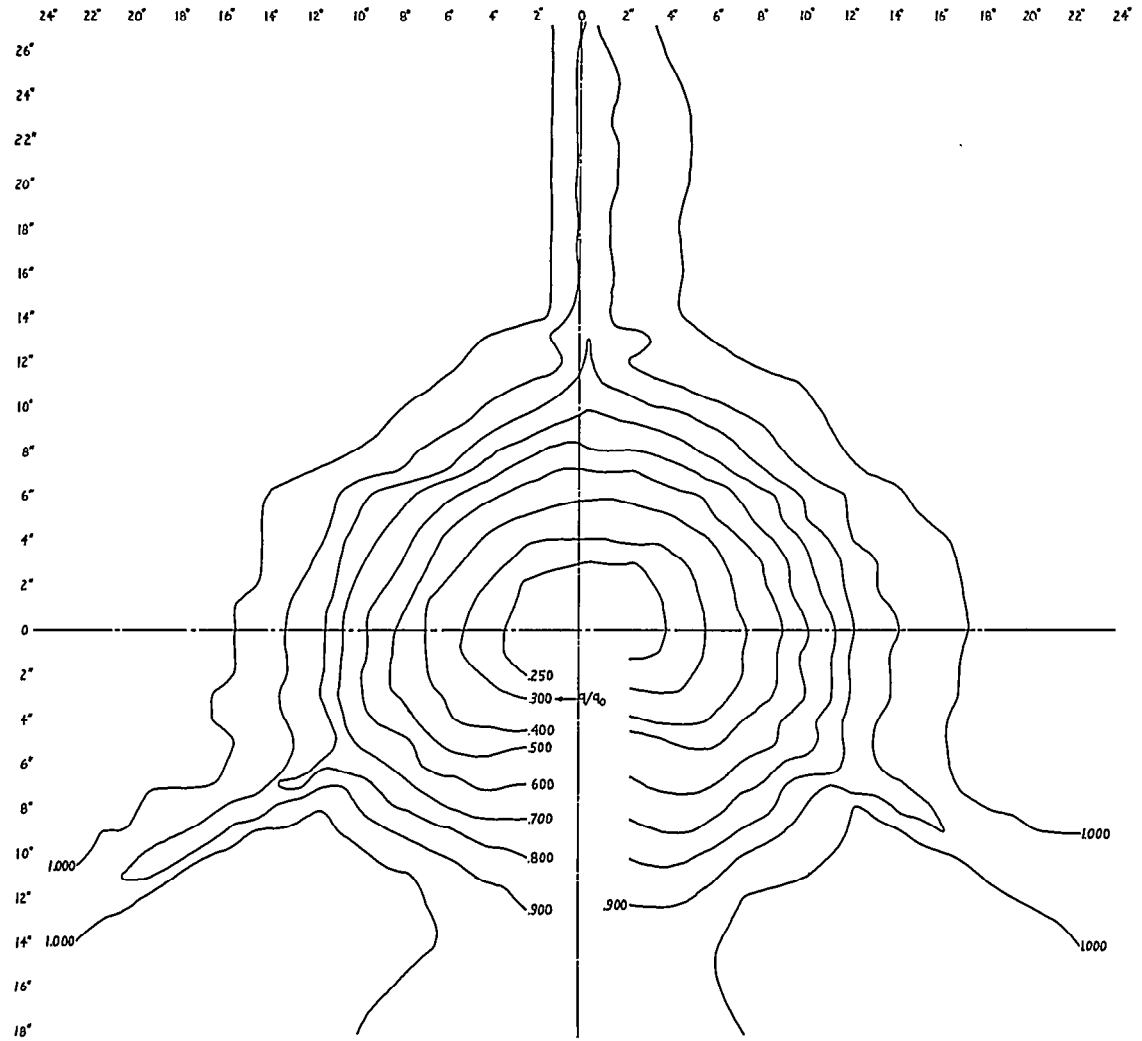

Figure 15.- Local dynamic-pressure-ratio variations in a plane normal to the stream and 1 inch behind the tail cone center. $\psi = 0^{\circ}$; $\alpha = 0^{\circ}$; $\delta_r = 0^{\circ}$; $\delta_{e_L} = 0^{\circ}$; $\delta_{e_R} = 0^{\circ}$.

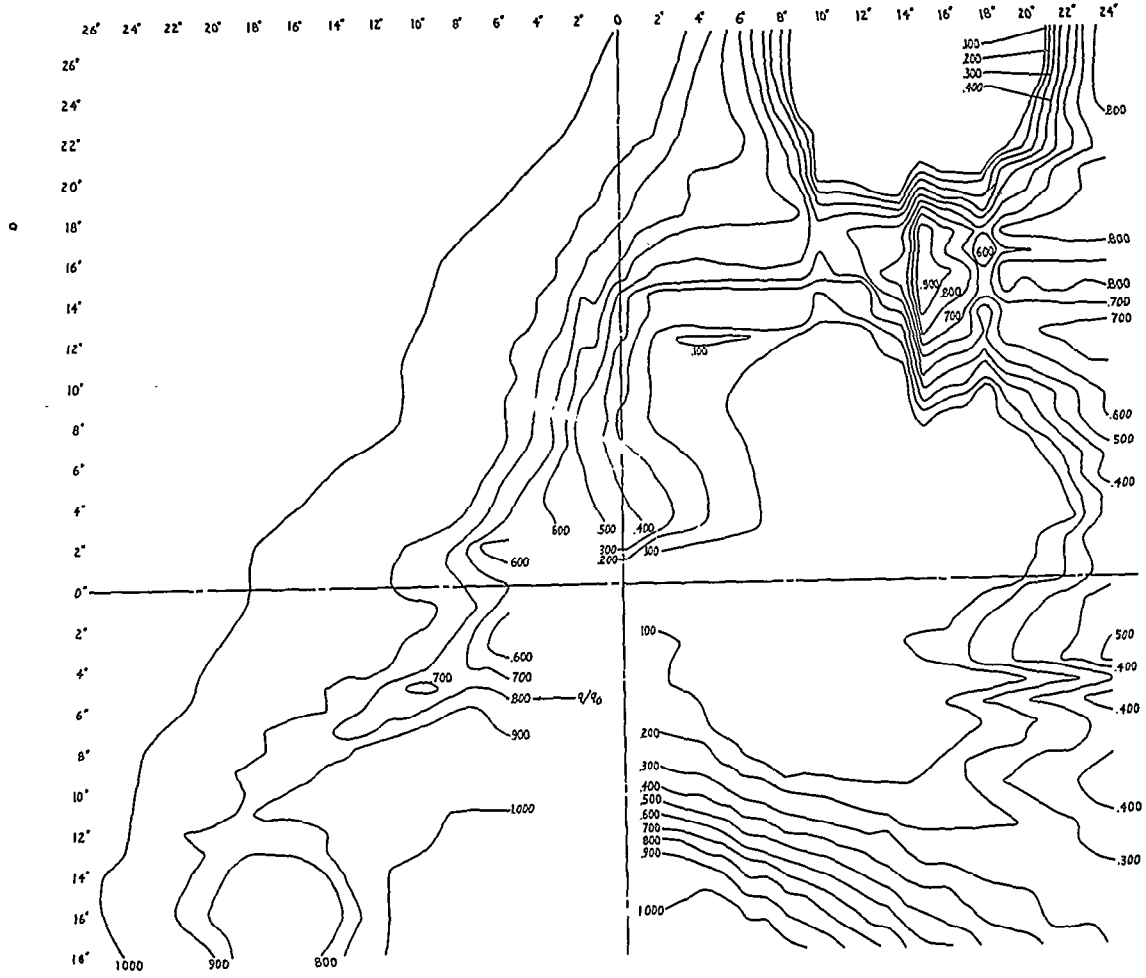

Figure 16.- Local dynamic-pressure-ratio variations in a plane normal to the stream. Origin of the coordinate system is the tail cone center projected $1\frac{3}{4}$ inches rearward along the hull axis. $\psi = 21^{\circ}$; $\alpha = 0^{\circ}$; $\delta_r = 0^{\circ}$; $\delta_{e_L} = 0^{\circ}$; $\delta_{e_R} = 0^{\circ}$.

NASA Technical Library
3 1176 01438 9754

[redacted]